MARMARA UNIVERSITY
INSTITUTE FOR GRADUATE STUDIES
IN PURE AND APPLIED SCIENCES

Design and Analysis of Robust Electromechanical Active Suspension Systems

Orhan Koray Çalık

MASTER THESIS

Department of Mechanical Engineering

Thesis Supervisor

Assoc. Prof. IBRAHIM SINA KUSEYRI

ISTANBUL, 2023

MARMARA UNIVERSITY
INSTITUTE FOR GRADUATE STUDIES
IN PURE AND APPLIED SCIENCES

Design and Analysis of Robust Electromechanical Active Suspension Systems

Orhan Koray Çalık
524619030

MASTER THESIS

Department of Mechanical Engineering

Thesis Supervisor

Assoc. Prof. IBRAHIM SINA KUSEYRI

ISTANBUL, 2023

MARMARA UNIVERSITY
INSTITUTE FOR GRADUATE STUDIES IN PURE AND APPLIED SCIENCES

Orhan Koray Çalık, a Master of Science student of Marmara University Institute for Graduate Studies in Pure and Applied Sciences, defended his thesis entitled "Design and Analysis of Robust Electromechanical Active Suspension Systems ", on January 2023 and has been found to be satisfactory by the jury members.

Jury Members

Doç. Dr. İbrahim Sina Kuseyri (Advisor)
Marmara University .....(SIGN).....

Doç. Dr. Mehmet Berke Gür (Jury)
Bahçeşehir University .....(SIGN).....

Prof. Dr. Bülent Ekici (Jury)
Marmara University .....(SIGN).....

APPROVAL

Marmara University Institute for Graduate Studies in Pure and Applied Sciences Executive Committee approves that Orhan Koray ÇALIK be granted the degree of Master of Science in Department of Mechanical Engineering, Mechanical Engineering Master Program on 2023 . (Resolution no:).

Director of the Institute
Prof. Dr. Bülent Ekici

ACKNOWLEDGEMENT

I would like to thank my thesis Advisor Assoc. Prof. İbrahim Sina KUSEYRI for taking the time to help and support me out through this thesis.

Last and most importantly, I present my deepest gratefulness to my mother Rukiye ÇALIK and, father Osman Nuri ÇALIK, for supporting me and my decisions and providing me all the tools and support that I need to complete my educations.Also, I am thankful my twin brother Burhan Turgay ÇALIK for moral support during my master education.

January 2023

Orhan Koray ÇALIK

(Mechanical Engineer)

Contents

ÖZET iv

ABSTRACT vi

SYMBOLS viii

ABBREVIATIONS xii

LIST OF FIGURES xiii

LIST OF TABLES xvi

1 INTRODUCTION 1

1.1 General Look to Suspension Technologies 2

1.2 Literature Survey 5

1.3 Objectives 8

2 VEHICLE SUSPENSION SYSTEM 9

2.1 Suspension System Main Concepts 10

2.1.1 Definition of Ride Comfort 11

2.1.2 Definition of Handling 12

2.1.3 Definition of Actuator Effort 13

2.2 Vehicle Suspension Models 13

2.2.1 Half-car Slow Active Vehicle Model 13

2.2.2 Half-car Full Active Vehicle Model 19

2.3 Road conditions 22

3 CONTROL OF ACTIVE SUSPENSION **24**

3.1 Control Objectives 24

3.2 H_∞ control 25

3.3 Controller synthesis model 26

3.4 Robustness Requirements 29

3.5 Weighting filters 29

3.5.1 Sprung accelerations 30

3.5.2 Tire compressions 30

3.5.3 Actuator effort 31

3.5.4 Suspension travel 32

4 RESULTS AND DISCUSSIONS **33**

4.1 Passive Suspension System Simulation Results 33

4.2 H_∞ Control Simulation Results 39

4.3 Evaluation of Simulations 56

5 CONCLUSION **60**

REFERENCES 61

6 APPENDIX **63**

6.1 Slow-active Half Car Suspension State-space Equation . . 63

6.2 Full-active Half Car Suspension State-space Equation . . . 67

6.3 PSD Graphs of Suspension Systems 71

ÖZET

GÜRBÜZ ELEKTROMEKANİK AKTİF SÜSPANSİYON SİSTEMLERİ TASARIMI VE ANALİZİ

Süspansiyon taşıtlarda sürüş konforu ve yol tutuşu üzerinde büyük etkisi olan bir sistemdir. Süspansiyon sistemi yol üzerindeki kavis ve engebelerden kaynaklı titreşimleri en aza indirmek görevlerin yerine getirir. Bu görevlere ek olarak viraj ve dönemeçlerde aracın kontrolünü arttırma görevini üstlenir. Sistem içerisindeki yaylar yardımıyla taşıtın yolla kesintisiz temasta olmasını ve yoldan gelen enerjinin depolanmasını sağlar. Sistem içerisinde bulunan amortisör yaya aktarılan enerjinin sönümlenmesi görevini yenine getirir. Ancak sadece yay ve amortisörden oluşan klasik süspansion sistemleri değişen ortam koşullarına uyum sağlayamamaktadır. Bu yüzden aktif ve yarı-aktif süspansiyon sistemleri geliştirilmiştir. Yarı-aktif süspansiyon sistemlerinde taşıtın sönümlenmesi amortisör içindeki elektrik kontrollü bir valfle gerçekleştirilir. Amortisör içindeki yağın viskositesinin ayarlanması sayesinde taşıt üzerindeki titreşim ve taşıtın yol tutuşu kontrol edilir. Bu tür süspansiyonlar dinamik sönümleme kontrollü sistemler olarak da adlandırılır. Aktif-süspansiyonlarda ise taşıtın sönümleme katsayısı ve katılığı hali hazırda buluna yay ve amortisörün yanına ek aktüatör eklenerek kontrol edilir. Bu sistemlerin amacı güvenlik ve sürüş konforunu birleştirmektir. Gelişen teknoloji ile aktif süspansiyon uygulamaları artmaktadır. Aktif süspansiyonlarda hidrolik, pnömatik ve elekromekanik aktüatörler kullanılmaktır. Bu tezde aktif süspansiyonun türleri olan full-aktif süspansiyon ve yavaş-aktif süspansiyon için gürbüz kontrolcüler tasarlanacaktır. Çalışmamızda H_∞ kontrol yaklaşımı kullanılmıştır. Kontrolcü optimizasyonuda kullanılacak sınırlayıcı faktörler dikey gövde ivmelenmesi, taşıt lastiği dinamik sıkışması, süspansiyon açıklığı

ve elektromeknik aktüatör çabasıdır. Çalışma sonucunda yavaş-aktif süspansiyonun full-aktif süspansiyona göre aktüatör çabası açısında avatajlı olduğu gözlemlenmiştir.

ABSTRACT

DESIGN AND ANALYSIS OF ROBUST ELECTROMECHANICAL ACTIVE SUSPENSION SYSTEMS

Suspension is a mechanism that has a significant impact on vehicle handling and comfort. The suspension system is responsible for reducing vibrations generated by road curves and bumps. Furthermore, the suspension system is in charge of improving vehicle control in bends and curves. The mechanism guarantees that the car maintains constant touch with the road, and the power from the road is stored using springs in the suspension. The shock absorber in the system, in turn, absorbs the energy that is transferred to the spring. Traditional suspension systems, which consist of a spring and a shock absorber, cannot adjust to changing environmental circumstances. As a result, active and semiactive suspension systems have been created. A semi-active suspension system regulates vehicle damping using a shock absorber controlled by an electric valve. The viscosity of the oil in the shock absorber is adjusted to control the vibration and handling of the vehicle.

These suspensions are also known as dynamic damping controlled systems. Furthermore, an active-suspension system, in addition to the existing spring and shock absorber, controls the damping coefficient and stiffness of the vehicle with the use of an additional actuator. The goal of these systems is to combine both safety and comfort while driving. Besides, the use of active suspensions is becoming more common as technology advances. In active suspensions applications, hydraulic, pneumatic, and electromechanical actuators are commonly employed. Robust controllers for full-active suspension and slow-active suspension, both types of active suspension, will be designed in this thesis. Robust control technique H_∞

control is applied in this study. Vertical body acceleration, tire dynamic compression, suspension clearance, and electromechanical actuator effort are all limiting variables in controller optimization. In terms of actuator effort, the simulation revealed that the slow-active suspension outperformed the full-active suspension.

SYMBOLS

c_{b_f} : Front suspension damping coefficient $[N/m]$

c_{b_r} : Rear suspension damping coefficient $[N/m]$

c_s : Body damping coefficient $[N/m]$

F_f : Force acting front of car body $[N]$

F_r : Force acting rear of car body $[N]$

F_{w_f} : Force acting front wheel $[N]$

F_{w_r} : Force acting rear wheel $[N]$

h : Roadway excitation $[m]$

h_f : Front roadway excitation $[m]$

h_r : Rear roadway excitation $[m]$

J_y : Pitch moment of inertia $[kg{\cdot}m^2]$

k_{b_f} : Front suspension stiffness $[N/m]$

k_{b_r} : Rear suspension stiffness $[N/m]$

k_s : Suspension stiffness $[N/m]$

k_{w_f} : Front tire stiffness $[N/m]$

k_{w_r} : Rear tire stiffness $[N/m]$

k_t : Tire stiffness $[N/m]$

l_f : Front wheelbase $[m]$

l_r : Rear wheelbase $[m]$

m_b : Quarter-car body mass $[kg]$

m_w : Quarter-car wheel mass $[kg]$

M_b : Half-car body mass $[kg]$

m_{w_f} : Front wheel mass $[kg]$

v : Longitudinal velocity of the vehicle $[m/s]$

ω_b : The natural frequency of the vehicle body $[rad/s]$

ω_w : Natural frequency of wheel $[rad/s]$

ω_d : The damped natural frequency of the vehicle body $[rad/s]$

$\omega_{0,act}$: Natural frequency of actuator $[rad/s]$

ω_{0,act_f} : Natural frequency of front actuator $[rad/s]$

ω_{0,act_r} : Natural frequency of rear actuator $[rad/s]$

z_{act_f} : Front actuator spring seat relative displacement $[m]$

z_{act_r} : Rear actuator spring seat relative displacement $[m]$

$\dot{z}_{act_f}$: Front actuator spring seat velocity [m/s]

$\dot{z}_{act_r}$: Rear actuator spring seat acceleration $[m/s^2]$

$\ddot{z}_{act_f}$: Front actuator spring seat acceleration $[m/s^2]$

$\ddot{z}_{act_r}$: Rear actuator spring seat velocity $[m/s]$

z_b : Vertical body displacement $[m]$

$\dot{z}_b$: Vertical body velocity $[m/s]$

$\ddot{z}_b$: Vertical body acceleration $[m/s^2]$

z_{b_f} : Front vertical body displacement $[m]$

z_{b_r} : Rear vertical body displacement $[m]$

z_w : Vertical wheel displacement $[m]$

z_{w_f} : Front vertical wheel displacement $[m]$

z_{w_r} : Rear vertical wheel displacement $[m]$

$\dot{z}_{w_f}$: Front vertical wheel velocity $[m/s]$

$\dot{z}_{w_r}$: Rear vertical wheel velocity $[m/s]$

$\ddot{z}_{w_f}$: Front vertical wheel acceleration $[m/s^2]$

$\ddot{z}_{w_r}$: Rear vertical wheel acceleration $[m/s^2]$

θ : Car body rotation angle $[rad]$

$\dot{\theta}$: Car body rotation velocity $[rad/s]$

$\ddot{\theta}$: Car body rotation acceleration $[rad/s^2]$

σ : Decaying constant

ζ : Damping ratio of LPF

u_f : Front actuator signal input

u_f : Rear actuator signal input

u'_f : Front LPF signal to perfect actuator

u'_r : Rear LPF signal to perfect actuator

ABBREVIATIONS

LPF :Low-pass filter

SAA :Slow-active actuator

RMS :Root mean squared

PSD :Power spectral density

MA :Maximum amplitude

LIST OF FIGURES

1.1 Citroën air hydractive suspension system 3

1.2 Bose active suspension system 4

2.1 Vehicle motions 9

2.2 Quarter car model 10

2.3 Human perception against certain disturbances 12

2.4 Half-car vehicle slow active suspension model 14

2.5 Half-car vehicle, full active suspension model 20

2.6 Road condition samples 23

3.1 General H_∞ control configuration 25

3.2 Plant and unmodeled dynamics 27

3.3 Model used for controller synthesis 28

3.4 5th order and 2nd order ISO 2631 weights 31

4.1 Passive suspension systems body linear acceleration based on road profiles 34

4.2 Passive suspension system body angular acceleration based on road profiles 35

4.3 Passive suspension system front suspension travel based on road profiles 36

4.4 Passive suspension system rear suspension travel based on road profiles 37

4.5 Passive suspension system front tire compression based on road profiles 38
4.6 Passive suspension system rear tire compression based on road profiles 39
4.7 H_∞ control linear acceleration on smooth road 40
4.8 H_∞ control linear acceleration on rough road 40
4.9 H_∞ control linear acceleration on bump 41
4.10 H_∞ control angular acceleration on smooth road 42
4.11 H_∞ control angular acceleration on rough road 42
4.12 H_∞ control angular acceleration on bump 43
4.13 H_∞ control front suspension travel on smooth road 44
4.14 H_∞ control front suspension travel on rough road 44
4.15 H_∞ control front suspension travel on bump 45
4.16 H_∞ control rear suspension travel on smooth road 46
4.17 H_∞ control rear suspension travel on rough road 46
4.18 H_∞ control rear suspension travel on bump 47
4.19 H_∞ control front tire compression on smooth road 48
4.20 H_∞ control front tire compression on rough road 48
4.21 H_∞ control front tire compression on bump 49
4.22 H_∞ control rear tire compression on smooth road 50
4.23 H_∞ control rear tire compression on rough road 50
4.24 H_∞ control rear tire compression on bump 51
4.25 H_∞ control front actuator effort on smooth road 52
4.26 H_∞ control front actuator effort on rough road 52

4.27 H_∞ control front actuator effort on bump 53
4.28 H_∞ control rear actuator effort on smooth road 54
4.29 H_∞ control rear actuator effort on rough road 54
4.30 H_∞ control rear actuator effort on bump 55

6.5 Passive suspension systems body linear acceleration PSD based on road profiles 71
6.6 Passive suspension system body angular acceleration PSD based on road profiles 71
6.7 H_∞ control linear acceleration PSD graph on smooth road . 72
6.8 H_∞ control linear acceleration PSD graph on rough road . . 72
6.9 H_∞ control linear acceleration PSD graph on bump 73
6.10 H_∞ control angular acceleration PSD graph on smooth road 73
6.11 H_∞ control angular acceleration PSD graph on rough road . 74
6.12 H_∞ control angular acceleration PSD graph on bump . . . 74

LIST OF TABLES

List of Tables

2.1 Vehicle Parameters 21

2.2 Road condition parameters 22

3.1 Uncertainty parameters of half car model 28

4.1 RMS values and PSD maximum amplitudes based on various road conditions for linear acceleration of car body for passive suspension system 34

4.2 RMS values and PSD maximum amplitudes based on various road conditions for angular acceleration of car body for passive suspension system 35

4.3 RMS values and PSD maximum amplitudes based on various road conditions for front suspension travel for passive suspension system 36

4.4 RMS values and PSD maximum amplitudes based on various road conditions for rear suspension travel for passive suspension system 37

4.5 RMS values and PSD maximum amplitudes based on various road conditions for front tire compression for passive suspension system 38

4.6 RMS values and PSD maximum amplitudes based on various road conditions for rear tire compression for passive suspension system 39

4.7 RMS values and PSD maximum amplitudes based on various road conditions linear body acceleration for slow-active and full-active suspensions controlled by H_∞ controller . . 41

4.8 RMS values and PSD maximum amplitudes based on various road conditions angular body acceleration for slow-active and full-active suspensions controlled by H_∞ controller 43

4.9 RMS values and PSD maximum amplitudes based on various road conditions front suspension travel for slow-active and full-active suspensions controlled by H_∞ controller . . 45

4.10 RMS values and PSD maximum amplitudes based on various road conditions rear suspension travel for slow-active and full-active suspensions controlled by H_∞ controller . . 47

4.11 RMS values and PSD maximum amplitudes based on various road conditions front tire compression for slow-active and full-active suspensions controlled by H_∞ controller . . 49

4.12 RMS values and PSD maximum amplitudes based on various road conditions rear tire compression for slow-active and full-active suspensions controlled by H_∞ controller . . 51

4.13 RMS values and PSD maximum amplitudes based on various road conditions front actuator effort for slow-active and full-active suspensions controlled by H_∞ controller . . 53

4.14 RMS values and PSD maximum amplitudes based on various road conditions rear actuator effort for slow-active and full-active suspensions controlled by H_∞ controller 55

4.15 Uncertainty rages result of μ-analysis of close-loop suspension systems 56
4.16 Comparison table of suspensions linear accelerations based on RMS and PSD values on smooth road condition 56
4.17 Comparison table of suspensions linear accelerations based on RMS and PSD values on rough road condition 56
4.18 Comparison table of suspensions linear accelerations based on RMS and PSD values on bump condition 57
4.19 Comparison table of suspensions angular accelerations based on RMS and PSD values on smooth road condition 57
4.20 Comparison table of suspensions angular accelerations based on RMS and PSD values on rough road condition 57
4.21 Comparison table of suspensions angular accelerations based on RMS and PSD values on bump condition 57
4.22 Comparison table of suspensions average tire compression based on RMS and PSD values on smooth road condition . 58
4.23 Comparison table of suspensions average tire compression based on RMS and PSD values on rough road condition . . 58
4.24 Comparison table of suspensions average tire compression based on RMS and PSD values on bump condition 58
4.25 Comparison table of suspensions average actuator effort based on RMS and PSD values on smooth road condition . 59
4.26 Comparison table of suspensions average actuator effort based on RMS and PSD values on rough road condition . . 59
4.27 Comparison table of suspensions average actuator effort based on RMS and PSD values on bump condition 59

1. INTRODUCTION

Suspension is a critical component of the chassis. The chassis is a term that refers to the structure of a vehicle and its components, which include the suspension system, wheels, brakes, and steering system. These components collaborate to carry out the functions of the chassis. In other words, these roles include ensuring the vehicle's structural integrity, protecting the driver and passengers from external forces, and providing ride comfort [7]. Among these components, the suspension system, which is the subject of this thesis, is constructed by vehicle subcomponents such as spring, damper, and tire, which define the vehicle's driving dynamics. The suspension system has a significant impact on vehicle handling, safety, and comfort [3].

Various suspension systems have been created to improve vehicle handling, safety, and comfort. These systems manage the vehicle's interface with the road as well as its response to it. These are known as active suspension systems that are categorized into semi-active and full-active suspension systems. The damper is controlled by semi-active suspension systems. It seeks to achieve the ideal driving characteristics by adjusting the suspension system's damping coefficient. In addition to the existing spring and damper components, full active suspension includes an actuator that runs parallel to the elements and delivers force to the system. As a result, the actuator regulates the stiffness and damping dynamics of the suspension. Slow active suspension systems can be thought of as a subset of active suspension systems, where the actuator in the slow active suspension system is connected in series to the spring in the system.

In active suspensions, several control techniques including as skyhook, PID, and LQR are used today. These approaches cannot ensure that active

suspension systems will perform as expected in all conditions and will not be influenced by disturbances and noises, this explains why active suspension control necessitates a strong control strategy. This research focuses on the robust control of full active and slow active suspension systems, as well as the performance comparison of these systems.

As a result, this research aims to demonstrate that the actuator effort of slow active suspension systems is superior to the actuator effort of complete active suspension systems without sacrificing driving comfort and safety. The H_∞ controller is created in this study. Systems with optimal performance and power consumption will be developed as a result of the robust control of suspension systems. The suspension control models employed in a computer simulation environment are also created, along with using a half-vehicle model. The goal is to achieve a more realistic simulation result than the quarter-vehicle model utilized in prior studies.

The system's performance is decided by the variables listed below. Driving comfort, (vehicle vertical acceleration), $|\ddot{z}_b|$, handling, (tire compression) $|z_w - h|$, and actuator effort $|u|$ are examples. The root-mean-square (RMS) and power spectral density (PSD) will be used to evaluate our variables [3].

1.1 General Look to Suspension Technologies

Many automotive manufacturers have been working on active suspension technology since the 1980s. Many examples of this technology can still be seen, such as active body control (ABC) by Mercedes and hydractive by Citroën. The different types of active suspension can be divided into two major categories: full-active suspension and semi-active suspension. In fact, the key distinction between these systems is the amount of power required for operation.

A semi-active system can adjust the damping of the system but cannot apply force to it, whereas a full-active system can supply force to the system in order to actively control it. Full active suspension systems contribute to the development of semi-active suspension systems, which commonly employ magneto-rheological systems. Mercedes active body control suspension consists of a spring, damper, and hydraulic actuator. The system bandwidth is 5 Hz and is mostly utilized for driving clearance vehicle management. The system runs at 200 bar pressure and consumes 3-5kW of power [2].

Citroën Air Hydractive is a system that employs a hydraulic diagram accumulator. The diagram is filled with nitrogen, and the amount of nitrogen is actively controlled by a pump and valves. Provided assistance can also alter riding characteristics and the ride level [15].

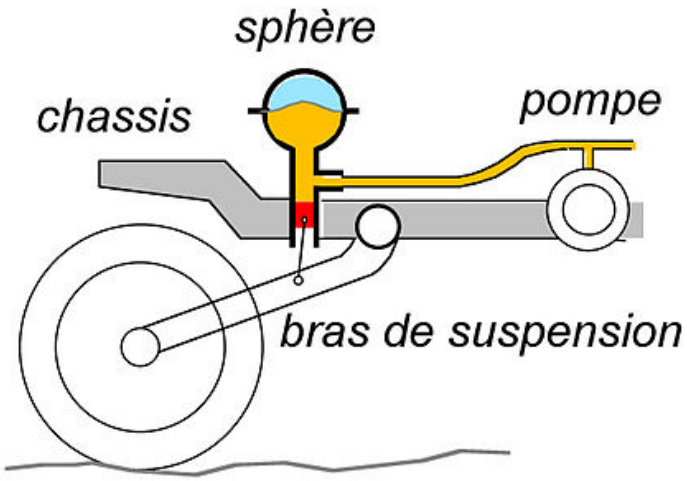

Figure 1.1: Citroën air hydractive suspension system

Delphi Technology employs a magnetic field with varying viscosity properties. According to the manufacturer, the system is probably changing 1000 times per second. Skyhook control can ensure good damping performance while consuming 5W less power than a hydraulic suspension system. Delphi technologies' system is used by Ferrari and Cadillac [1].

Bose Corporation created a suspension system that demands signifi-

cant power consumption but does not have the restrictions of a hydraulic actuator suspension system. The technology employs an electromagnetic actuator to achieve high bandwidth while also being capable of energy regeneration. The device, according to the maker, can stabilize roll and pitch motions while cornering and braking.



Figure 1.2: Bose active suspension system

1.2 Literature Survey

Known as hydro-pneumatic suspension, Citroën brought active suspension in the 1950s. In the 1970s, researchers began to investigate active suspensions. Then, various publications, aimed at actively regulating the suspension, were published.

The study "Robust design of active suspension system" published in 1993 [11], focused on the quarter car suspension concept. When the system is defined with parametric uncertainties, the study demonstrates the drawbacks of the LQR control strategy. When unknown parameters have various nominal conditions, the system produces an unwanted response. The author, in order to accomplish objective behavior on the system using the state feedback H_∞ control strategy, compensates for parametric uncertainty impacts at the expense of system performance. With only a few trials, the system reaches the requisite level of robustness.

Der Sande's [3] robust control approach is applied to a practical electromagnetic actuator full active quarter car system. The robust controller design incorporates metric and nonparametric uncertainty. As a result, the author created a LQG controller with no robust attributes for comparison reasons. The author compares and contrasts simulated and measured controllers. When obtaining the necessary degree of robustness and performance.

Vehovers [14] simulates road conditions by referencing velocity roughness and terrain elements and employing a variety of active suspension controller designs for quarter vehicle models, including LQG, full state feedback, and skyhook. Then, examines the performance of the controllers.

Kabil's master thesis [7], titled "Alternative control techniques for electromechanical active suspension system" models a low bandwidth (Slow) active suspension system to achieve desired suspension performance and

ride comfort. The system is designed to control the actuator in a variety of ways, including skyhook, groundhook, complete state feedback, and combinations. The systems were then tested in both a virtual and real-world context. The analysis concludes that the best controller is a combination of skyhook and state-space control.

The goal of "Preview Control of Slow Active Suspension System" [4] is to model and control a slow active suspension system that is adaptable to a half-car model. The actuator dynamics are also modeled as a second-order low pass filter by the authors. The author designed many controllers to accomplish desired ride comfort and suspension deflection utilizing various control methodologies such as LQG and preview control. The author then examined systems with controller effects on the system based on the desired performance goals.

Soyici [13] employs LMI optimization for the goal of designing a controller for the quarter vehicle model that employs a combination of H_2 and H_∞ performance criteria. The author's goal is to keep suspension while minimizing vertical body acceleration and to keep the deflection within a specific boundary. For acquiring the appropriate H_2 and H_∞ mixed controller, the author analyses the data using (RMS) root-mean-square values.

Researchers at the University of Pretonia [6] worked on several automotive models such as quarter, half, and complete car models. The researchers obtained each system dynamic and simulated these systems in a computer environment. The simulation data are then compared to measurement data from the numerous sensors used to evaluate the car. The results suggest that more thorough modeling brings us closer to simulation and measurement data. Researchers also investigated the value of vertical acceleration. With measurement data, the entire car model exhibited a similar value. Then, using data from closeness measurements, other car models align. The half-car model yielded the second-best close data, and the final model

was the quarter automobile.

Koch [8] developed on the quarter-vehicle model, which was evaluated on stochastic road profiles and discontinuous disturbance events like bumps. For suspension systems, the author employed skyhook, adaptive skyhook, and LQR techniques. The suspension workbench was then tested by the author. The author compared each system's performance.

Additionally, many authors have thought about employing LQG and skyhook control methods. This study, in turn, on synthesis of a robust control strategy. The approach will then be applied to the half-car model, since more accurate computer simulation results than the quarter-car model are desired. The control technique will use a slow active and a complete, active half-car model to demonstrate how a slow active system requires less actuator effort than a full active system while sacrificing little ride comfort and handling performance.

1.3 Objectives

The electromechanical suspension has several advantages, these advantages can be seen in having lower energy consumption when compared to hydraulic and pneumatic systems, the absence of the need for additional equipment to keep the system running efficiently, and having simplified system maintenance. As a result, in this study, the actuator type for slow and full active suspension systems is used for controlling the suspension model. In addition, the goal of this research is to demonstrate slow and full active suspension systems with powerful control techniques. The benefits and drawbacks of these systems will then be examined in order to achieve balanced controller ride comfort and actuator effort.

In other words, the study's objectives can be described in several steps:

- Modeling a slow and full active suspension system by using MATLAB that includes electromechanical actuator dynamics.
- Creating the test conditions, such as roads with the properties of smooth, rough, and bumpy roads.
- Creating filters for this study-related controller synthesis, such as one for modifying acceleration, suspension travel, and actuator effort.
- Simulating the systems using previously provided inputs such as smooth, rough, and bumpy road conditions.
- Clarifying the processing system replies by comparing performance using multiple approaches such as root-mean-square (RMS) values and power spectral density analysis.

2. VEHICLE SUSPENSION SYSTEM

A suspension system can be used to describe system components as dampers, springs, and reduces vibrations on a vehicle. This system responds to various critical vehicle functions such as providing ride comfort, modifying driving characteristics, and controlling the car's roll, pitch, and yaw behavior. The vehicle body and passengers are also protected from disturbances that are caused by road conditions, which affect the yaw, pitch, and roll dynamics of the vehicle body. Furthermore, the suspension system has the ability to keep the wheels connected to the road surface for power transmission, handling, acceleration, and braking, all of which have a direct impact on driving safety.

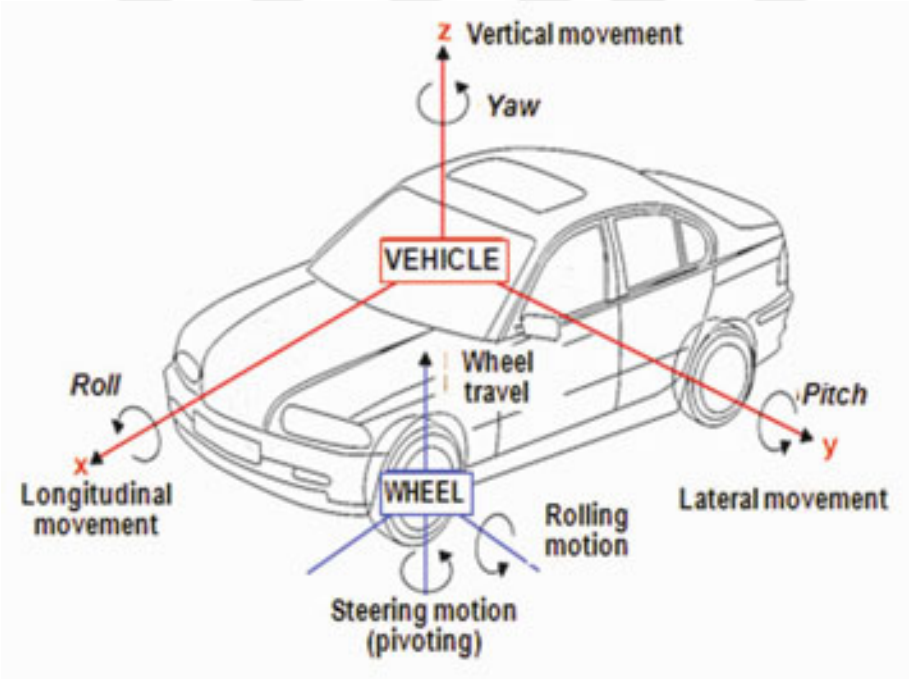

Figure 2.1: Vehicle motions

The figure shows us the motions capable of car chassis which affect car stability and safety.

2.1 Suspension System Main Concepts

The suspension system's major effect is to reduce vibration. This vibration is created by source road stimulation that is transmitted to the wheels and subsequently to the chassis via the suspension system, where the elements spring and damper interact with one another. The properties of a spring are determined by the degree of compression and tension, as well as the measurement of the damper's reaction speed. Both pieces limit the vertical displacement of the chassis. A vehicle's attributes influence its comfort and handling. These are the underlying frequencies of the chassis and wheels.

Besides, the damper in the suspension system guarantees that the amplitude of the oscillation is reduced. The natural frequencies of the car body and wheel are different. The simplest suspension model, the quarter-car model, can be used to demonstrate these features.

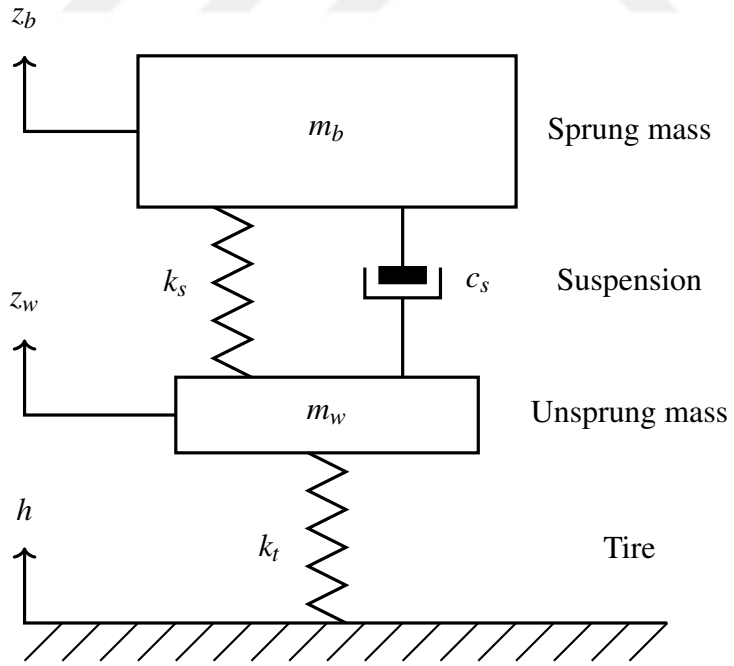

Figure 2.2: Quarter car model

The natural frequency of the car body can be calculated as follows [7]:

$$\omega_b = \sqrt{\frac{k_b}{m_b}} \tag{2.1}$$

The natural frequency of the wheel can be calculated as follows [7]:

$$\omega_w = \sqrt{\frac{k_b + k_t}{m_w}} \tag{2.2}$$

The system possesses decaying oscillations features such as decay rate 'σ' and damped frequency 'ω_d' because of the damping element of the system. The equations are shown in equations (2.3) and (2.4) [7].

$$\sigma = \frac{c_s}{m_b} \tag{2.3}$$

$$\omega_d = \sqrt{{\omega_n}^2 - \sigma^2} \tag{2.4}$$

2.1.1 Definition of Ride Comfort

Passengers' riding comfort is affected by disturbance vibration. This vibration is caused by part excitations on the road and in the powertrain. To prevent disturbances of this kind, the suspension system is quite significant. Additionally, ride comfort can determine vertical and angular acceleration parameters of the car body.

Vertical acceleration is represented by $|\ddot{z}_b|$, and angular acceleration is represented by $|\ddot{\theta}|$. Root Mean Square (RMS) and Power Spectral Density (PSD) values are measured and compared. The comfort concept is founded on human perception, as evidenced by various scientific studies. These studies point to a frequency range of 4-8 Hz that is bothersome to humans

[3].

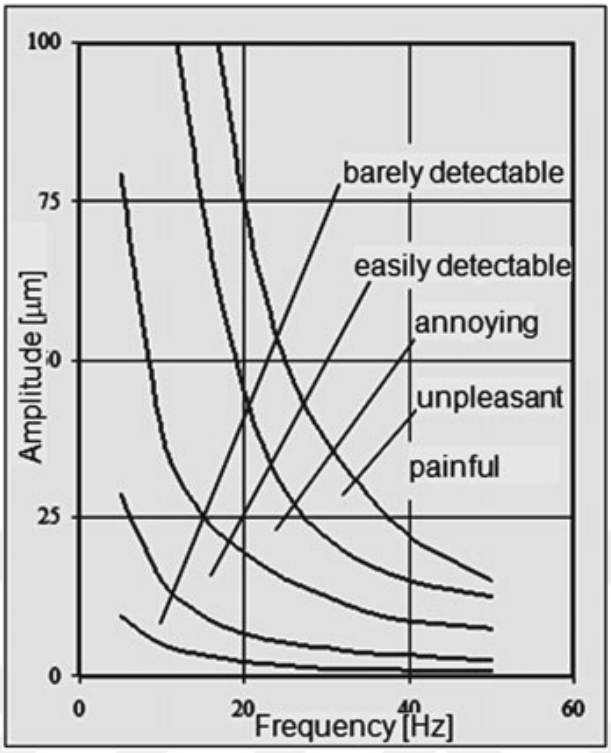

Figure 2.3: Human perception against certain disturbances

2.1.2 Definition of Handling

Vehicle handling is essential when performing actions such as steering, accelerating, and braking. The force between the tire and the road influences handling. The force affects two primary factors: the unstrung wheel and the body that causes vibrations. General admission, as well as stiff tire signifies a reduced dynamic tire help force to better handling performance. Tire sidewall thickness and tire pressure are two tire parameters that might affect handling.

Moreover, the interface between the road and the tire is critical for understanding the concept. To illustrate, for the half-car vehicle model, the compression value of each tire, which represents $|z_{w_f} - h_f|$ for the front tire and $|z_{w_r} - h_r|$ for the rear tire, may simply be obtained. For a safe drive, the values while driving must be lower than certain recognized val-

ues. Similarly to acceleration values, the values measure and compare root-mean-square (RMS) and power spectral density (PSD) data [3].

2.1.3 Definition of Actuator Effort

Actuator effort is defined as the energy of signal flow from the controller to the actuator. This term has a direct impact on the active suspension system's power consumption. The Root Mean Square and Power Spectral Density value can be used to evaluate the signal.

2.2 Vehicle Suspension Models

2.2.1 Half-car Slow Active Vehicle Model

This car model has four degrees of freedom. The motion of car body is evaluated in terms of pitch and heave. Figure 2.4 shows a schematic illustration of the model. The model is included slow active actuators that were modeled using linear parameters. The system is composed of three rigid bodies: the vehicle body, the front, and rear wheel assemblies.

Several assumptions underlie the system:

- The vehicle is driven horizontally at a constant speed.
- The vehicle has the ability to move vertically.
- Wheel assemblies allow for vertical movement.
- The suspension system is thought to exert force point interactions through the vehicle body.
- Tire stiffness represents by linear springs.
- The vehicle is exposed to road disturbances caused by road irregularities.

- The suspension system actuators are founded between the car body and wheel assemblies to apply force.

The system's degrees of freedom are as follows:

- The vertical travel of the vehicle's center of mass
- The rotating movement of the vehicle's body mass center
- The vertical travels of the front and rear wheel assemblies

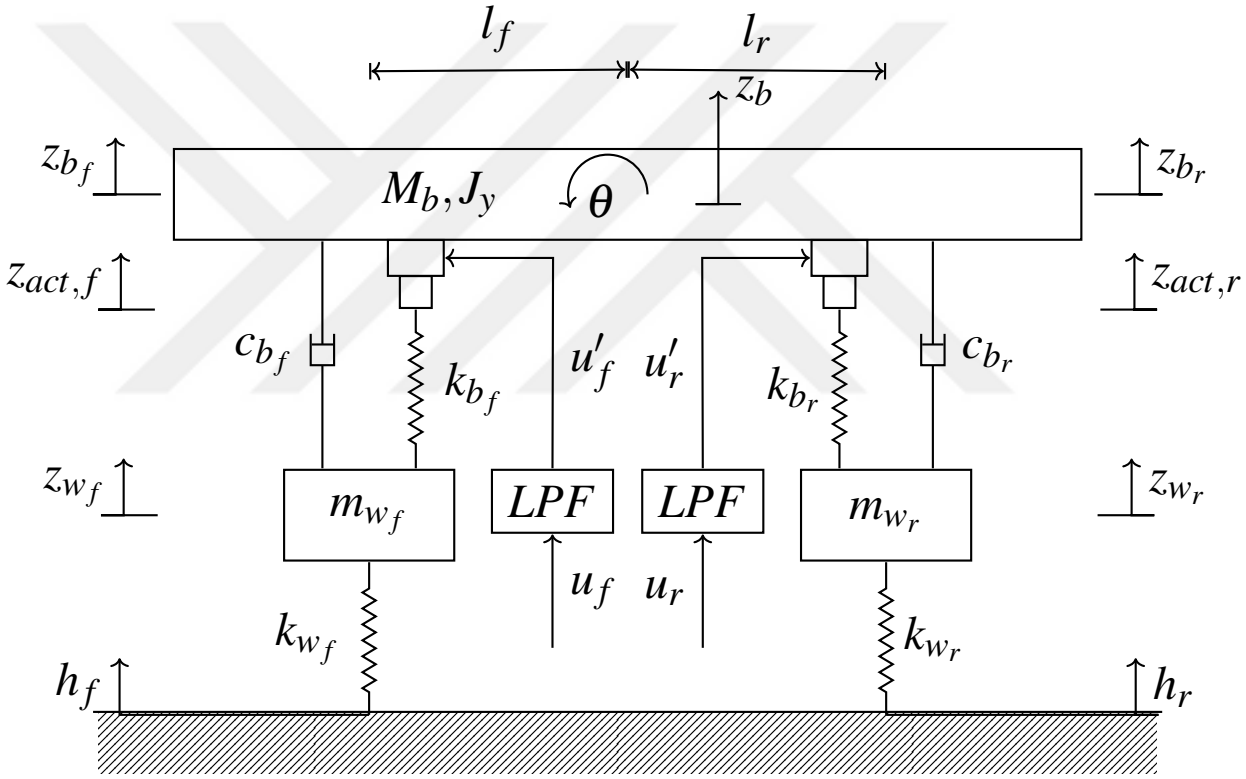

Figure 2.4: Half-car vehicle slow active suspension model

A slow-active actuator system consists of an actuator with a limited bandwidth coupled in series to a spring and in parallel to a damper. The system is an example of a displacement control problem. A second order low pass filter, which is coupled to the ideal actuator, can simulate the actuator's typical limited bandwidth [4].

A generic form of low-pass filter can be defined using by the equation (2.5). The input and the output signals are defined by x and y, respectively. The constant parameters are $\omega_{0,act}$, natural frequency of and actuator ζ damping ratio of LPF.

$$\ddot{y} + 2\zeta\,\omega_{0,act}\dot{y} + {\omega_{0,act}}^2 y = {\omega_{0,act}}^2 x \tag{2.5}$$

The forces acting on the car body can be defined using the dynamic equation (2.6).

$$M_b\ddot{z}_b = -F_f - F_r \tag{2.6}$$

Torques act on the car body can also be defined, along with the dynamic equation, using equation (2.7).

$$J_y\ddot{\theta} = l_f F_f - l_r F_r \tag{2.7}$$

In (2.8) equations, the forces acting on each wheel assembly are represented.

$$m_{w_f}\ddot{z}_{w_f} = F_f - F_{w_f} \tag{2.8a}$$

$$m_{w_r}\ddot{z}_{w_r} = F_r - F_{w_r} \tag{2.8b}$$

In equations (2.9) and (2.10), the forces are rewritten in terms of spring and damper elements. Slow-active variables are represented by $z_{act,f}$ and $z_{act,r}$. actuator (SAA) displacements in terms of z_{b_f} and z_{b_r} positions.

$$F_f = k_{b_f}(z_{act,f} - z_{w_f}) + c_{b_f}(\dot{z}_{b_f} - \dot{z}_{w_f}) \tag{2.9a}$$

$$F_r = k_{b_r}(z_{act,r} - z_{w_r}) + c_{b_r}(\dot{z}_{b_r} - \dot{z}_{w_r}) \tag{2.9b}$$

$$F_{w_f} = k_{w_f}(z_{w_f} - h_f) \tag{2.10a}$$

$$F_{w_r} = k_{w_r}(z_{w_r} - h_r) \tag{2.10b}$$

The parameters of z_{b_f} and z_{b_r} are redefined in terms of z_b and θ in equations .

$$z_{b_f} = z_b - l_f\theta \tag{2.11a}$$

$$z_{b_r} = z_b + l_r\theta \tag{2.11b}$$

The previous equations are summed up in the following equations (2.12), (2.13), (2.14), and (2.15).

$$\begin{aligned}\ddot{\theta} = \frac{1}{J_y}[(-{l_f}^2 c_{b_f} - {l_r}^2 c_{b_r})\dot{\theta} + (l_f c_{b_f} - l_r c_{b_r})\dot{z}_b - l_f k_{b_f} z_{w_f} \\ -l_f c_{w_f}\dot{z}_{w_f} + l_r k_{b_r} z_{b_r} + l_r c_{b_r}\dot{z}_{w_r} + l_f k_{b_f} z_{act,f} - l_r k_{b_r} z_{act,r}]\end{aligned} \tag{2.12}$$

$$\begin{aligned}\ddot{z}_b = \frac{1}{M_b}[(l_f c_{b_f} - l_r c_{b_r})\dot{\theta} - (c_{b_f} + c_{b_r})\dot{z}_b + k_{b_f} z_{w_f} + c_{b_f}\dot{z}_{w_f} \\ +k_{b_r} z_{w_r} + c_{b_r}\dot{z}_{w_r} - k_{b_f} z_{act,f} - kb_r z_{act,r}]\end{aligned} \tag{2.13}$$

$$\ddot{z}_{w_f} = \frac{1}{m_{w_f}}[-l_f c_{b_f}\dot{\theta} + c_{b_f}\dot{z}_b - (k_{b_f} + k_{w_f})z_{w_f} - c_{b_f}\dot{z}_{w_f} + k_{b_f} z_{act,f} + k_{w_f} h_f] \tag{2.14}$$

$$\ddot{z}_{w_r} = \frac{1}{m_{w_r}}[l_r c_{b_r}\dot{\theta} + c_{b_r}\dot{z}_b - (k_{b_r} + k_{w_r})z_{w_r} - c_{b_r}\dot{z}_{w_r} + k_{b_r} z_{act,r} + k_{w_r} h_r] \tag{2.15}$$

Second-order LPF equations are defined in equations (2.16).

$$\ddot{u}'_f + 2\zeta\omega_{0,act_f}\dot{u}'_f + \omega^2_{0,act_f} u'_f = \omega^2_{0,act_f} u_f \tag{2.16a}$$

$$\ddot{u}'_r + 2\zeta\omega_{0,act_r}\dot{u}'_r + \omega^2_{0,act_r} u'_r = \omega^2_{0,act_r} u_r \tag{2.16b}$$

Equations (2.17) is defined by the system actuator input.

$$u'_f = z_{b_f} - z_{act,f} \tag{2.17a}$$

$$u'_r = z_{b_r} - z_{act,r} \tag{2.17b}$$

The conventions of z_{b_f} and z_{b_r} to z_b and θ result in the (2.18) equations.

$$u'_f = z_b + l_f\theta - z_{act,f} \tag{2.18a}$$

$$u'_r = z_b - l_r\theta - z_{act,r} \tag{2.18b}$$

Then, $\ddot{z_{act},f}$ and $\ddot{z_{act},r}$ are taken the derivative twice.

$$\ddot{z_{act},f} = \ddot{z}_b + l_f\ddot{\theta} - \ddot{u}'_f \tag{2.19a}$$

$$\ddot{z_{act},r} = \ddot{z}_b - l_r\ddot{\theta} - \ddot{u}'_r \tag{2.19b}$$

(2.20) and (2.21) are the final actuator dynamics equations. LPF dynamics were also used to embed the equations.

$$\begin{aligned}\ddot{z}_{act,f} = &-l_f w_{0,act_f}^2\theta + (-2l_f w_{0,act_f} + l_f c_{b_f}a_1 - l_r c_{b_r}a_2)\dot{\theta} + w_{0,act_f}^2 z_b \\ &+(2\zeta w_{0,act_f} - c_{b_f}a_1 - c_{b_r}a_2)\dot{z}_b + k_{b_f}a_1 z_{b_f} + c_{b_f}a_1\dot{z}_{b_f} + k_{b_r}a_2 z_{b_r} + c_{b_r}a_2\dot{z}_{b_r} \\ &-(w_{0,act_f}^2 + k_{b_f}a_1)z_{act,f} - 2\zeta w_{0,act_f}\dot{z}_{act,f} - k_{b_r}a_2 z_{act,r} - w_{0,act_f}^2 u_f\end{aligned} \tag{2.20}$$

$$\begin{aligned}\ddot{z}_{act,r} = &\, l_r w_{0,act_f}^2\theta + (2l_r w_{0,act_r} + l_f c_{b_f}a_2 - l_r c_{b_r}a_3)\dot{\theta} + w_{0,act_r}^2 z_b \\ &+(2\zeta w_{0,act_r} - c_{b_f}a_2 - c_{b_r}a_3)\dot{z}_b + k_{b_f}a_2 z_{b_f} + c_{b_f}a_2\dot{z}_{b_f} + k_{b_r}a_3 z_{b_r} \\ &+c_{b_r}a_3\dot{z}_{b_r} - k_{b_f}a_2 z_{act,f} - (w_{0,act_r}^2 + k_{b_r}a_3)z_{act,r} - 2\zeta w_{0,act_r}\dot{z}_{act,r} - w_{0,act_r}^2 u_r\end{aligned} \tag{2.21}$$

where

$$a_1 = \frac{1}{M_b} + \frac{l_f^2}{J_y}, a_2 = \frac{1}{M_b} - \frac{l_f l_r}{J_y}, a_3 = \frac{1}{M_b} + \frac{l_r^2}{J_y} \tag{2.22}$$

The system of state-space states are defined in vector (2.23).

$$\begin{aligned}z_s = [&\theta \quad \dot{\theta} \quad z_b \quad \dot{z}_b \quad z_{w_f} \quad \dot{z}_{w_f} \quad z_{w_r} \quad \dot{z}_{w_r} \quad z_{act,f} \quad \dot{z}_{act,f} \\ &z_{act,r} \quad \dot{z}_{act,r}]^T\end{aligned} \tag{2.23}$$

The disturbance and control inputs are defined in vectors (2.24).

$$w_i = [h_f \quad h_r]^T \tag{2.24a}$$

$$u_i = [u_f \quad u_r]^T \tag{2.24b}$$

The state-space system performance and measurement outputs are defined in vectors (2.25).

$$z_o = [z_{w_f} - h_f \quad z_{w_r} - h_r \quad \ddot{z}_b \quad \ddot{\theta} \quad z_{b_f} - z_{w_f} \quad z_{b_r} - z_{w_r} \quad u_f \quad u_r] \tag{2.25a}$$

$$y_o = [\ddot{z}_b \quad \ddot{\theta} \quad \ddot{z}_{w_f} \quad \ddot{z}_{w_r} \quad z_{b_f} - z_{w_f} \quad z_{b_r} - z_{w_r} \quad \dot{\theta}] \tag{2.25b}$$

The performance outputs are defined front tire compression $z_{w_f} - h_f$, rear tire compression $z_{w_r} - h_r$, vehicle body vertical acceleration $\ddot{z}_b$, vehicle body rotational acceleration $\ddot{\theta}$, front suspension travel $z_{b_f} - z_{w_f}$, rear suspension travel $z_{b_r} - z_{w_r}$, front actuator effort u_f, rear actuator effort u_r.

The measurement outputs are defined vehicle acceleration of vehicle body $\ddot{z}_b$, rotational acceleration of the vehicle body $\ddot{\theta}$, front wheel vertical acceleration $\ddot{z}_{w_f}$, rear wheel vertical acceleration $\ddot{z}_{w_r}$, front suspension travel $z_{b_f} - z_{w_f}$, rear suspension travel $z_{b_r} - z_{w_r}$, vehicle body rotational velocity $\dot{\theta}$.

2.2.2 Half-car Full Active Vehicle Model

The full active half-car system is seen in figure 2.5. The model is equipped with full active actuators and characterized by linear parameters. The model carries the same mechanical principles and assumptions as the previous slow-active half-car model. Also, The degrees of freedom of the suspension system is the same as the previous subsection model. The difference between the models originated from the actuator type and the connection style of actuator.

To control the vehicle, the full-active actuator incorporates a parallel-connected damper and spring. The actuator dynamics are represented with a first order transfer function which are limit of displacement 0.05 m. The full active actuator transfer function is modeled because represents rapid response behavior. The transfer function of the actuator is shown in equation (2.26) [10].

$$Actf,r = \frac{1}{1+s/60} \tag{2.26}$$

The dynamic equations of the system are written in terms of the vertical and angular movement of the vehicle body (2.27) and (2.28).

$$\begin{aligned} M_b\ddot{z}_b = -(c_{b_{f+c_{b_r}}})\dot{z}_b + (l_f c_{b_f} - l_r c_{b_r})\dot{\theta} - k_{b_f}(z_{b_f} - z_{w_f}) + c_{b_f}\dot{z}_{w_f} \\ -k_{b_r}(z_{b_r} - z_{w_r}) + c_{b_r}\dot{z}_{w_r} + u_f + u_r \end{aligned} \tag{2.27}$$

$$\begin{aligned} J_y\ddot{\theta} = (l_f c_{b_f} - l_r c_{b_r})\dot{z}_b - (l_f^2 c_{b_f} + l_r^2 c_{b_r})\dot{\theta} + l_f k_{b_f}(z_{b_f} - z_{w_f}) - l_f c_{b_f}\dot{z}_{w_f} \\ -l_r k_{b_r}(z_{b_r} - z_{w_r}) + l_r c_{b_r}\dot{z}_{w_r} - l_f u_f + l_r u_r \end{aligned} \tag{2.28}$$

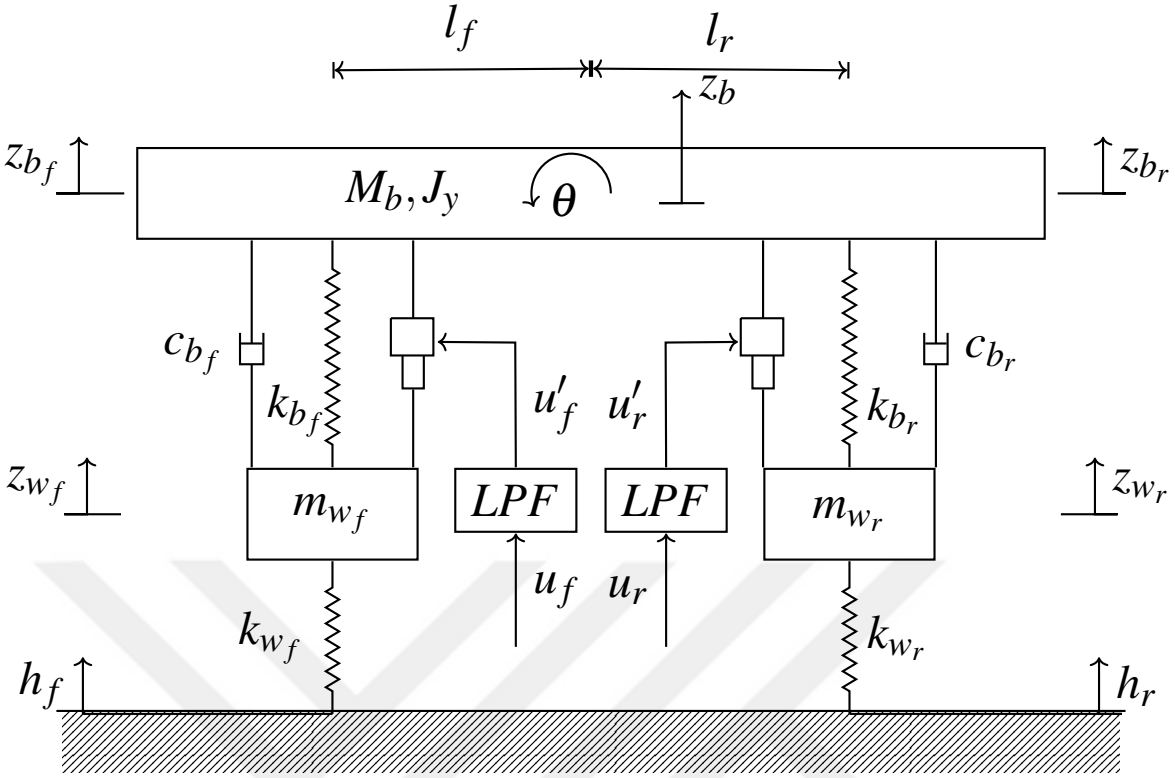

Figure 2.5: Half-car vehicle, full active suspension model

Equations (2.29) and (2.30) are obtained in terms of front and rear wheel masses.

$$\ddot{z}_{w_f} = -\frac{k_{w_f}}{m_{w_f}}z + \frac{c_{b_f}}{m_{w_f}}\dot{z} + \frac{l_f k_{w_f}}{m_{w_f}}\theta - \frac{l_f c_{b_f}}{m_{w_f}}\dot{\theta} + \frac{k_{b_f}+k_{w_f}}{m_{w_f}}(z_{b_f}-z_{w_f}) - \frac{c_{b_f}}{m_{w_f}}\dot{z}_{w_f} + \frac{k_{w_f}}{m_{w_f}}h_f - \frac{u_f}{m_{w_f}} \tag{2.29}$$

$$\ddot{z}_{w_r} = -\frac{k_{w_r}}{m_{w_r}}z + \frac{c_{b_r}}{m_{w_r}}\dot{z} - \frac{l_r k_{w_r}}{m_{w_r}}\theta + \frac{l_r c_{b_r}}{m_{w_r}}\dot{\theta} + \frac{k_{b_r}+k_{w_r}}{m_{w_r}}(z_{b_r}-z_{w_r}) - \frac{c_{b_r}}{m_{w_r}}\dot{z}_{w_r} + \frac{k_{w_r}}{m_{w_r}}h_r - \frac{u_r}{m_{w_r}} \tag{2.30}$$

The system of state-space states are defined in vector (2.31).

$$z_s = [z_b \quad \dot{z}_b \quad \theta \quad \dot{\theta} \quad z_{b_f}-z_{w_f} \quad \dot{z}_{w_f} \quad z_{b_r}-z_{w_r} \quad \dot{z}_{w_r}] \tag{2.31}$$

The disturbance and control inputs are defined in vectors (2.32).

$$w_i = [h_f \quad h_r]^T \tag{2.32a}$$

$$u_i = [u_f \quad u_r]^T \tag{2.32b}$$

The state-space system performance and measurement outputs are defined in vectors (2.33).

$$z_o = [z_{w_f} - h_f \quad z_{w_r} - h_r \quad \ddot{z}_b \quad \ddot{\theta} \quad z_{b_f} - z_{w_f} \quad z_{b_r} - z_{w_r} \quad u_f \quad u_r] \tag{2.33a}$$

$$y_o = [\ddot{z}_b \quad \ddot{\theta} \quad \ddot{z}_{w_f} \quad \ddot{z}_{w_r} \quad z_{b_f} - z_{w_f} \quad z_{b_r} - z_{w_r} \quad \dot{\theta}] \tag{2.33b}$$

The system inputs and outputs are the same as in the previous slow-active half-car model. Table 2.1 defines the slow-active and full-active vehicle suspension system parameters.

Table 2.1: Vehicle Parameters

Parameters	Symbol	Value
Half car mass $[kg]$	M_b	997
Front wheel mass $[kg]$	m_{w_f}	40
Rear wheel mass $[kg]$	m_{w_r}	40
Front wheel base $[m]$	l_f	1.2963
Rear wheel base $[kg]$	l_r	1.6477
Front suspension spring stiffness $[N/m]$	k_{b_f}	111000
Rear suspension spring stiffness $[N/m]$	k_{b_r}	67000
Front suspension damping coefficient $[Ns/m]$	c_{b_f}	3500
Rear suspension damping coefficient $[Ns/m]$	c_{b_r}	2800
Front tire stiffness $[N/m]$	k_{w_f}	234000
Rear tire stiffness $[N/m]$	k_{w_r}	234000
Car pitch moment of inertia $[kg{\cdot}m^2]$	J_y	3800
Slow-active actuators natural frequency $[rad/s]$	$w_{act,0_{f,r}}$	5.8
Slow-active actuators damping ratio [-]	ζ	0.9

2.3 Road conditions

While driving, a vehicle is subjected to disturbances. The disturbance has two essential characteristics: stochastic disturbance (random probability) and deterministic disturbance. The driving conditions, such as road surface quality, are described by stochastic disturbance. A first order filter that takes white noise as its input is represented in the road surface [9].

$$\frac{1}{vV_x}\dot{h} + h = w \tag{2.34}$$

Here, h is the vertical road heave, V_x is the vehicle's horizontal speed, and w is a white noise signal. The value v represents the cut-off frequency at which irregularities. The amplitude of the road condition is multiplied by ψ gain. t_s is defined sampling time and is defined 0.0025 s [3].

Table 2.2: Road condition parameters

Road type	$v(rad/m)$	$V_x(m/s)$	ψ
Smooth	0.2	30	$0.05\sqrt{\frac{0.001}{t_s}}$
Rough	0.8	7.5	$0.125\sqrt{\frac{0.001}{t_s}}$

The bumpy road condition is generated by in terms of a cos function, which defines equation (2.35) and is dependent on the t parameter. The function specifies a maximum bump of 0.03 meter height [10].

$$h = 0.015(1 - \cos(8\pi t)) \tag{2.35}$$

Our suspension systems are built around a half-car vehicle model. To demonstrate the characteristic, a delay between the front and rear wheel road disturbances is added. The delay is determined by the horizontal speed of the vehicle. The following equation (2.36) is used to describe the relation.

$$t_d = \frac{lf + lr}{V_x} \tag{2.36}$$

Figure 2.6 depicts sample road disturbance signals.

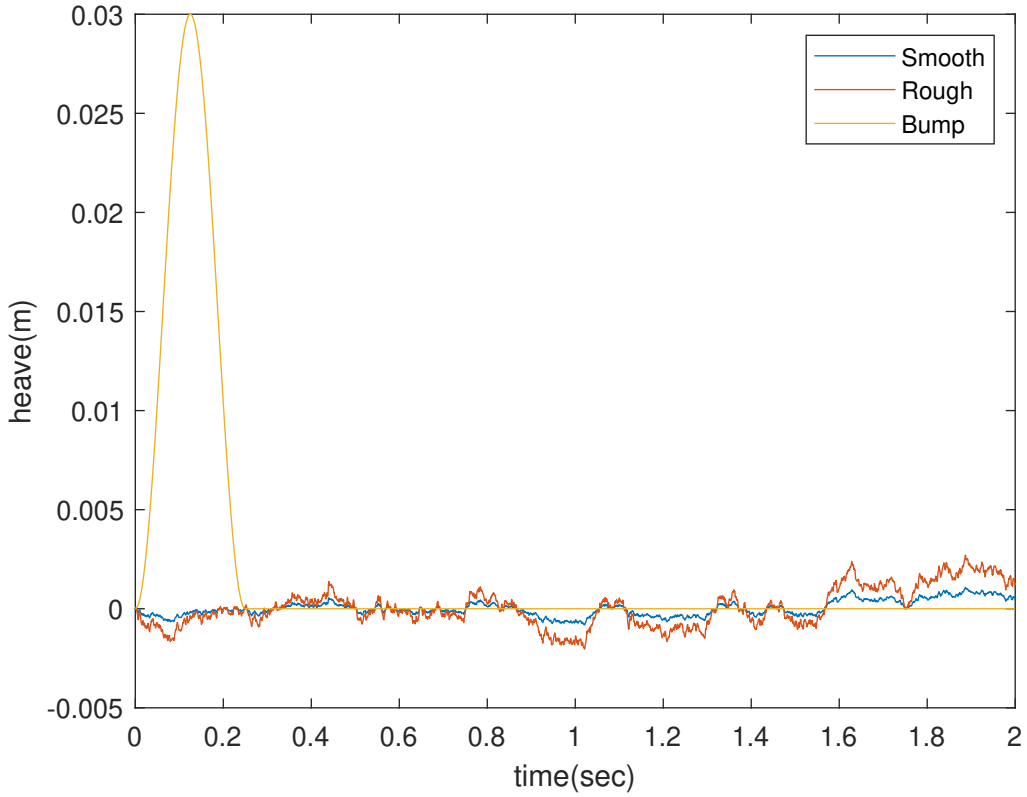

Figure 2.6: Road condition samples

3. CONTROL OF ACTIVE SUSPENSION

The preceding chapter introduced the slow-active and full-active half-car suspension. These system attributes will be utilized by the controllers. The chapter will concentrate on creating a controller to deal with random and bump inputs. Controllers will employ a robust control approach H_∞ when constructing the controller.

3.1 Control Objectives

The main control objectives of ride comfort, in this study, are defined by RMS and PSD vertical acceleration $\ddot{z}_b$. In order to improve ride comfort, the value will be compared to the ISO261 criterion. The ISO2631 target function approximated Zuo's fifth order transfer function [16].

$$W_{ISO2631} = \frac{87.72s^4 + 1138s^3 + 11336s^2 + 5453s + 5509}{s^5 + 92.69s^4 + 2550s^3 + 25969s^2 + 81057s + 79783} \quad (3.1)$$

The handling objective is also defined by the RMS tire compression of $z_{w_f} - h_f$ and $z_{w_r} - h_r$ for minimization of these variables, which maximize the vertical and horizontal forces acting on the vehicle wheels.

The suspension travels $z_{b_f} - z_{w_f}$ and $z_{b_r} - z_{w_r}$ are constrained by the suspension system's physical properties. The actuator-assisted suspension travel adjustment must be less than the maximum suspension clearance.

The end goal is actuator effort, which is obtained by RMS and PSD values.Actuator effort are demonstrated the energy advantage of slow-active versus full-active suspension systems.

3.2 H_∞ control

H_∞ method is used to synthesize a controller to achieve stabilization and desired performance.To use the method, system represent a general plant structure for applying mathematic optimization method of H_∞. Any H_∞ control problem is formulated as figure 3.1. $P(s)$ is linear system is defined as follows:

$$\begin{pmatrix} z \\ y \end{pmatrix} = P(s) \begin{pmatrix} w \\ u \end{pmatrix} = \begin{pmatrix} P_{11}(s) & P_{12}(s) \\ P_{21}(s) & P_{22}(s) \end{pmatrix} \begin{pmatrix} w \\ u \end{pmatrix} \tag{3.2}$$

The controller K is described in equation (3.3).

$$u = K(s)y \tag{3.3}$$

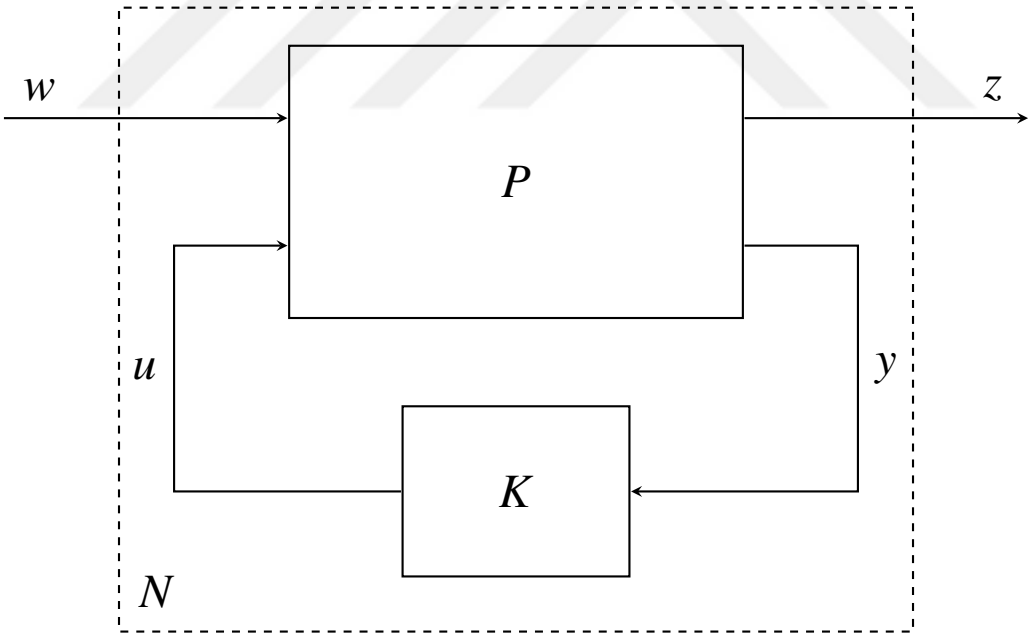

Figure 3.1: General H_∞ control configuration

The transfer function between z and w is represented with N.

$$z = T_{zw}(P,K)w = N(s)w \tag{3.4}$$

The lower linear transformation is used to define the N transfer function.

$$N(s) = T_{zw} = P_{11}(s) + P_{22}(s)K(s)[I - P_{22}(s)K(s)]^{-1}P_{21}(s) \tag{3.5}$$

Determine a controller K that stabilizes P given a generalized plant. N is also defined. The H_∞ norm of the transfer function matrix $N(s)$ is defined as:

$$||N(s)|| = ||T_{zw}(s)||_\infty = max_\omega \overline{\sigma}[T_{zw}(j\omega)] \tag{3.6}$$

Where ω is the maximum singular value of the matrix N($j\omega$).H_∞ norm of N should be small as possible.

$$||N||_\infty \leq \gamma \tag{3.7}$$

3.3 Controller synthesis model

The half vehicle model is used to design the robust controller that is similar to the models discussed in Chapter 2. Model uncertainties and weighting filters, however, must incorporate. The model depicted in Figure (3.3). The model's uncertainty can come from a variety of sources.

The system parameters of linear model are frequently estimated or incorrect. Furthermore, these parameters lack any non-linear characteristics such as damping coefficients.

Because of sensor noise or discretization, signal measurement is not ideal, which results in the fact that signals are uncertain. This uncertainty is represented in the table 3.1 by adding white noises with different gains.

Because of the lower degree model, the system's high frequency modes remain unknown. The system's degree of modeling the higher order modal frequencies can make the system unpredictable.

Instead of an excessively complex model, a less complex model be used, and the dynamics that were neglected be represented as uncertainty.

The controller that is implemented may differ from the one to appear by resolving the synthesis problem. To account for controller order reduction, some uncertainty could be included.

Furthermore, it is assumed that the system's dynamics are unknown; above 30 Hz. As illustrated in figure 3.2, a multiplicative uncertainty is thus introduced.

$$P_p = P(I + W_{unmodel}\Delta_I) \tag{3.8}$$

The system consists of uncertain vehicle mass, tire stiffness, and damping characteristics that fluctuate within a specified range.

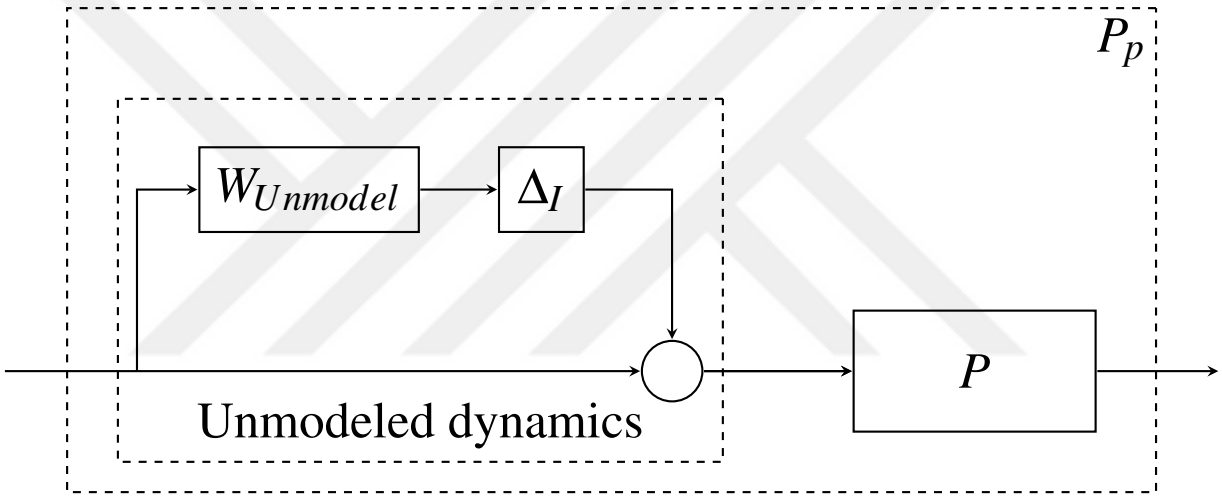

Figure 3.2: Plant and unmodeled dynamics

$W_{unmodel}$ can define as

$$W_{Unmodel} = \frac{\frac{1}{(2\pi 30)^2}s^2 + \frac{1.414}{2\pi 30} + 1}{\frac{1}{(2\pi 400)^2}s^2 + \frac{1.414}{2\pi 400} + 1} \tag{3.9}$$

W_{n1} to W_{n7} weights, repressed effect of random noises act on system. Front and rear tire compression, sprung vertical and rotational accelerations, front and rear suspension travel, and front and rear actuator effort are the eight weighted parameters utilized in H_∞ control.

Table 3.1: Uncertainty parameters of half car model

Parameter name	Uncertainty type	Mean value	Deviation
Sprung mass	Parametric uncertainty	997 kg	-85 +150 kg
Tire stiffness	Parametric uncertainty	2.34e5 N/m	$\pm$0.3e5 N/m
Front damping coefficient	Parametric uncertainty	3500 Ns/m	-550 +250 Ns/m
Rear damping coefficient	Parametric uncertainty	2800 Ns/m	-550 +250 Ns/m
Sprung vertical acceleration sensor	Sensor noise	-	$\pm 0.024 m/s^2$ RMS
Sprung angular acceleration sensor	Sensor noise	-	$\pm 0.024 rad/s^2$ RMS
Unsprung vertical acceleration sensor	Sensor noise	-	$\pm 0.178 m/s^2$ RMS
Suspension travel sensor	Sensor noise	-	$\pm 0.002 m$ RMS

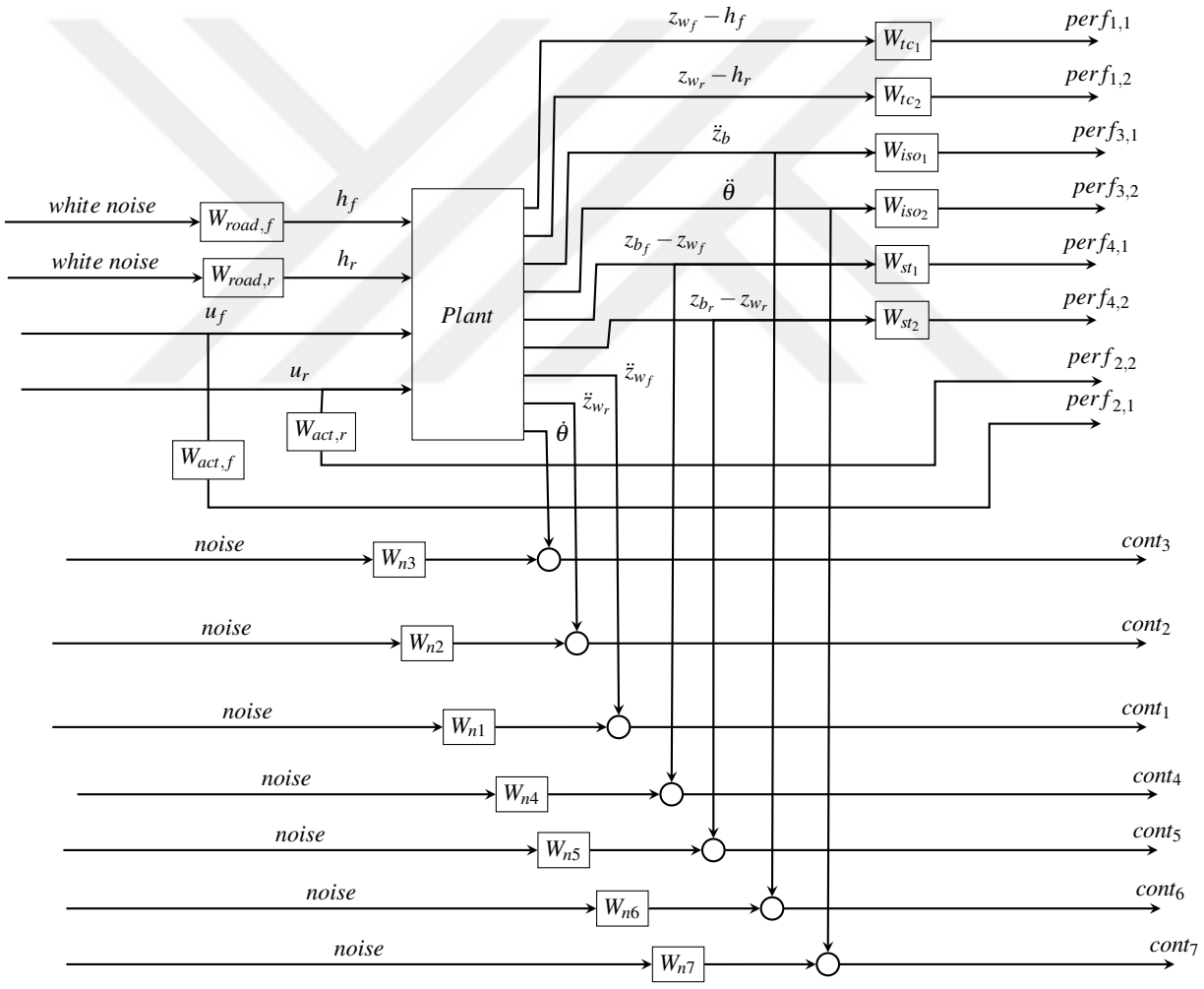

Figure 3.3: Model used for controller synthesis

3.4 Robustness Requirements

The controlled system's main requirements are performance and stability. Nominal Stability (NS) and Robust Stability (RS) are two categories under the stability requirement (RS). Nominal stability is obtained in system poles. All system poles must be left half plane. Furthermore, when robust stability is guaranteed, the controlled system is stable for all disturbed plants. The $N\Delta$ structure is taken into account in this, as shown in figure 3.2. The transfer function between exogenous inputs u and outputs y is defined as.

$$F_u(N,\Delta) = N_{22} + N_{21}\Delta(I - N_{11}\Delta)^{-1}N_{21} \tag{3.10}$$

N_{22} is the nominal plant, and N_{11} is the plant to link to the disturbances. Also, N must be stable, as $(I - N_{11}\Delta)^{-1}$ is the only source of instability. $M = N_{11}$ structure is stable, according to the Nyquist criterion. $M\Delta$ must be for all ω

$$\mu(M(j\omega)) < 1, \forall\omega \tag{3.11}$$

With μ the structured singular value.

3.5 Weighting filters

Weighting filters are used to shape input signals such as road disturbance and controller signals in order to accomplish performance goals. In addition, the size and design of performance filters can influence the frequency response of the outputs.

3.5.1 Sprung accelerations

Humans are particularly sensitive to vertical vibrations between 4 and 10 Hz. The ISO2631-1 standard for evaluating suspension performance takes this into account. Transfer function (3.12) shows Zuo's [16] achievement in transforming this frequency-dependent weighting into a continuous time transfer function for use in simulation. Despite the fact that up to fifth-order fits have been obtained, it was chosen to use the second order fit, which is defined as

$$W_{\ddot{z}_s}(s) = w_{\ddot{z}_s} \frac{86.51s + 546.1}{s^2 + 82.17s + 1892} \tag{3.12}$$

using $w_{\ddot{z}_s}$ a gain that is used to alter the importance of sprung acceleration. The use of this weighted filter has the disadvantage of having a very low gain at high frequencies, which allows for significant vertical acceleration and leads to instability. $w_{\ddot{z}_s}$ will be adjusted during the simulation process.

3.5.2 Tire compressions

Tire compression is widely used in the literature to indicate how well an automobile holds the road. This is a plausible assumption because the amount of lateral force a tire can create is affected by the vertical load. Pacejka's tire model is utilized to get the appropriate weight ([12]). The estimated first order filter is defined as

$$W_{z_t}(s) = w_{z_t} \frac{\frac{1}{2\pi 12}s + 1}{\frac{1}{2\pi 0.6}s + 1} \tag{3.13}$$

Because comfort is likely to be prioritized above minor sideslip angles when building weighted filters, allowing for more vertical displacement at higher frequencies, which will be similar to how the weighting filter

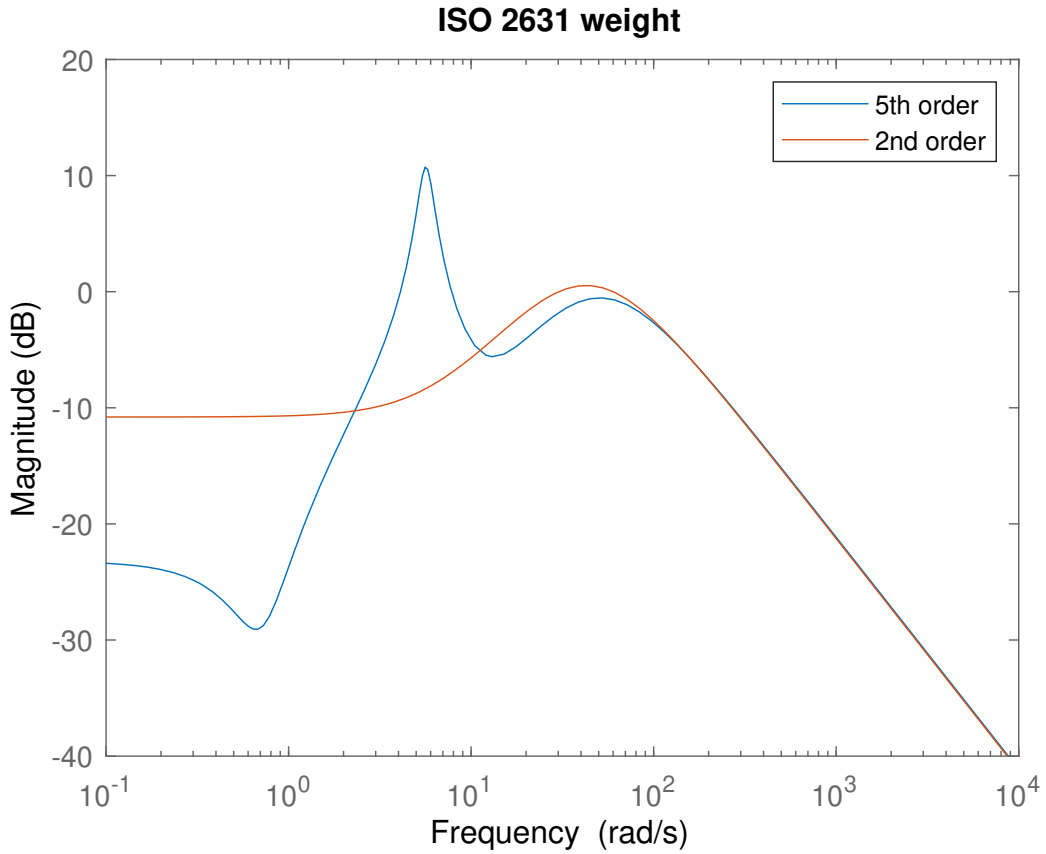

Figure 3.4: 5th order and 2nd order ISO 2631 weights

operates. In this application, w_{z_t} is a gain factor that can be utilized to highlight dynamic tire compression.

3.5.3 Actuator effort

The actuator's design positions its limits outside the frequencies of interest to maximize comfort and reduce actuator effort. The actuator parameters R and L, as well as the motor constants, were provided by Gysen [5]. However, there is no gain in comfort or handling at such frequency, the actuator is not necessary to apply force up to this frequency. Because tire and chassis resonances can occur over 30 Hz, it was determined to limit the actuator force above this frequency. The weighted filter, in turns, produces

a second-order, restricted high pass filter.

$$W_{Fact}(s) = w_{Fact} \frac{\frac{1}{(2\pi 30)^2}s^2 + \frac{2\beta_1}{2\pi 30}s + 1}{\frac{1}{(2\pi 200)^2}s^2 + \frac{2\beta_2}{2\pi 200}s + 1} \tag{3.14}$$

β_1 and β_2 are defined $\frac{1}{\sqrt{2}}$ as achieving smooth roll on and roll off. The actuator weighting filter's significance can be stated using the gain w_{Fact}.

3.5.4 Suspension travel

The suspension travel weight requirement is determined by the clearance between the sprung and unsprung masses. The gain is represented by a single gain that adjusts during simulation.

$$W_z(s) = w_z \tag{3.15}$$

4. RESULTS AND DISCUSSIONS

The simulation results are presented in this section. To achieve the best possible riding comfort, the optimum control settings for each controller model were first determined in the previous chapter. As a result, multiple simulations are done using various controller types to understand the reaction of the controller. The controller models created in MATLAB aid in the development of the control system toolbox and the robust control toolbox.

4.1 Passive Suspension System Simulation Results

The simulation model of the passive suspension system does not create actuator motions. The simulation is tested the vehicle's response to the road conditions which are defined in chapter 2, and these measurements are utilized as baseline comparison data. These measurements are the vehicle's linear and angular accelerations, suspension travels, tire compression, and actuator efforts.

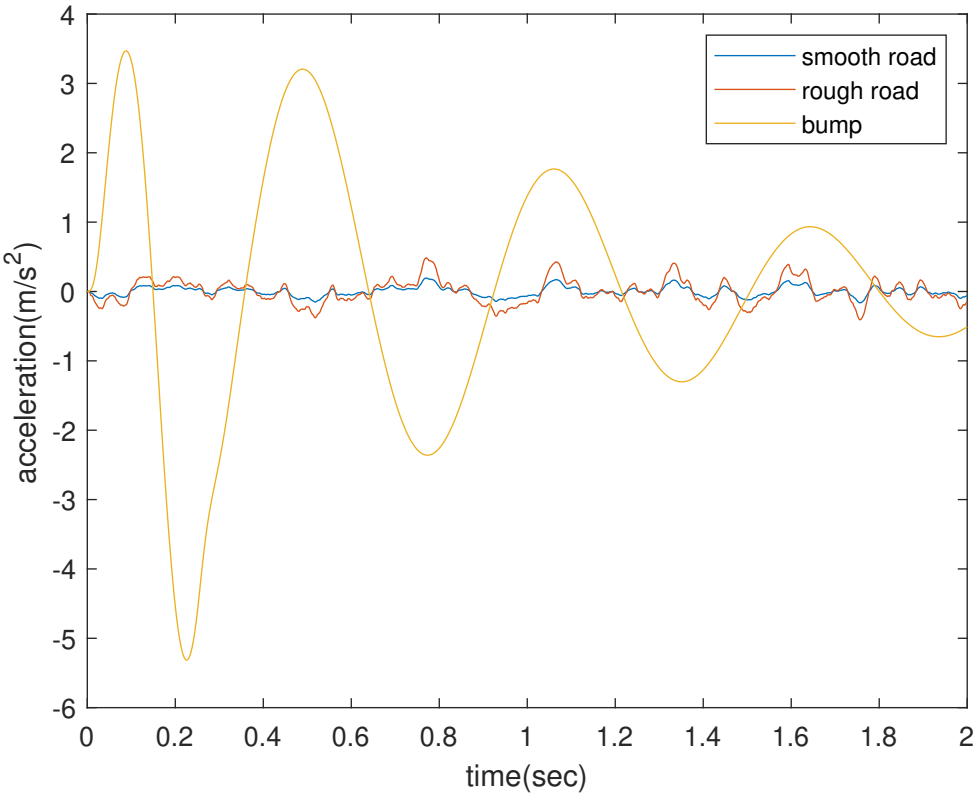

Figure 4.1: Passive suspension systems body linear acceleration based on road profiles

	RMS Value $[m/s^2]$	PSD maximum amplitude $[dB/Hz]$
smooth road	0.0782	0.0045
rough road	0.1904	0.0317
bump	1.7734	5.65

Table 4.1: RMS values and PSD maximum amplitudes based on various road conditions for linear acceleration of car body for passive suspension system

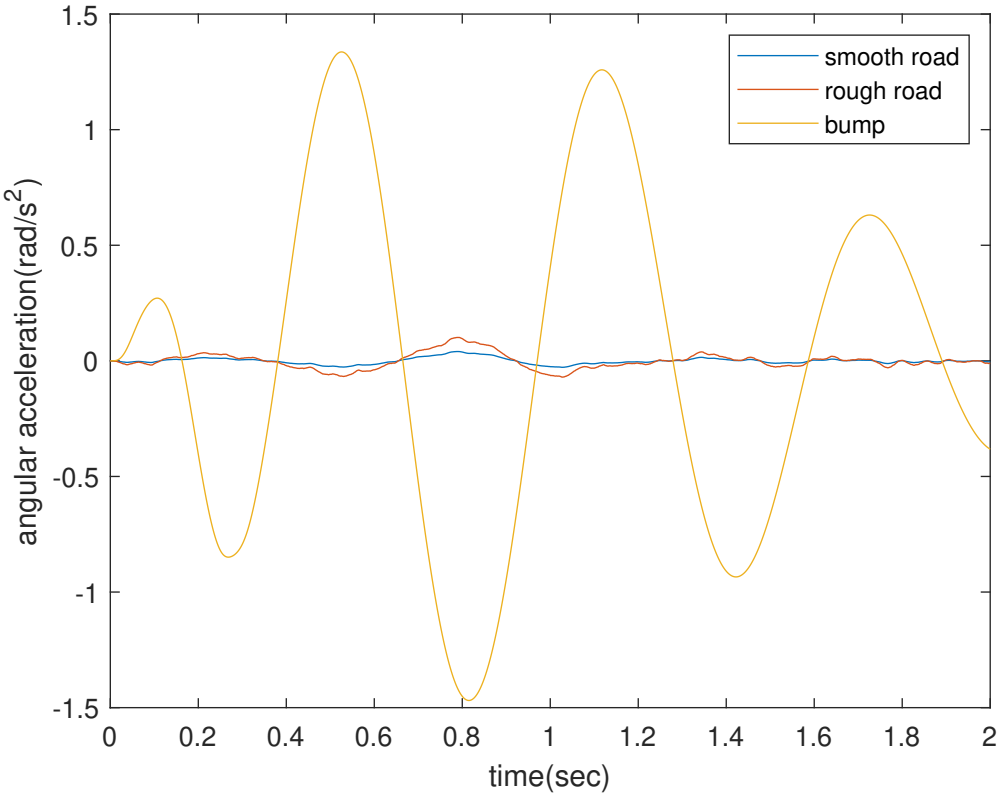

Figure 4.2: Passive suspension system body angular acceleration based on road profiles

	RMS Value $[rad/s^2]$	PSD Maximum Amplitude $[dB/Hz]$
smooth road	0.0134	$3.0529x10^{-4}$
rough road	0.0335	0.0019
bump	0.7440	1.3724

Table 4.2: RMS values and PSD maximum amplitudes based on various road conditions for angular acceleration of car body for passive suspension system

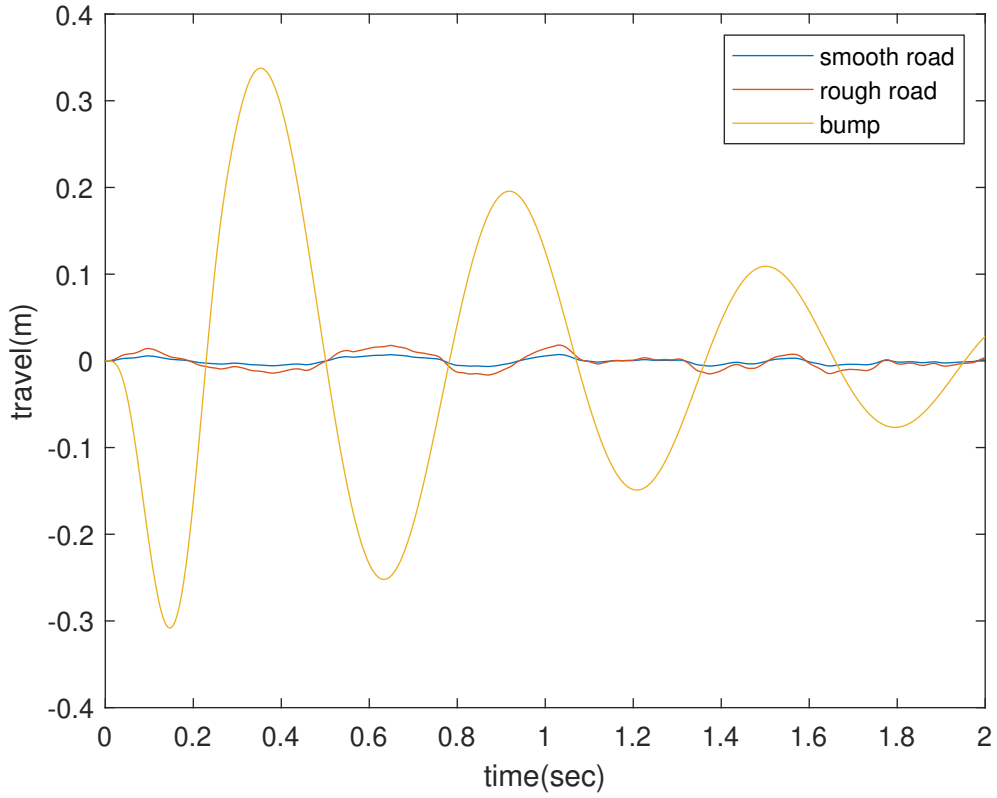

Figure 4.3: Passive suspension system front suspension travel based on road profiles

	RMS Value $[m]$	PSD maximum amplitude $[dB/Hz]$
smooth road	0.0036	$2.1804x10^{-5}$
rough road	0.0091	$1.3642x10^{-4}$
bump	0.1489	0.0403

Table 4.3: RMS values and PSD maximum amplitudes based on various road conditions for front suspension travel for passive suspension system

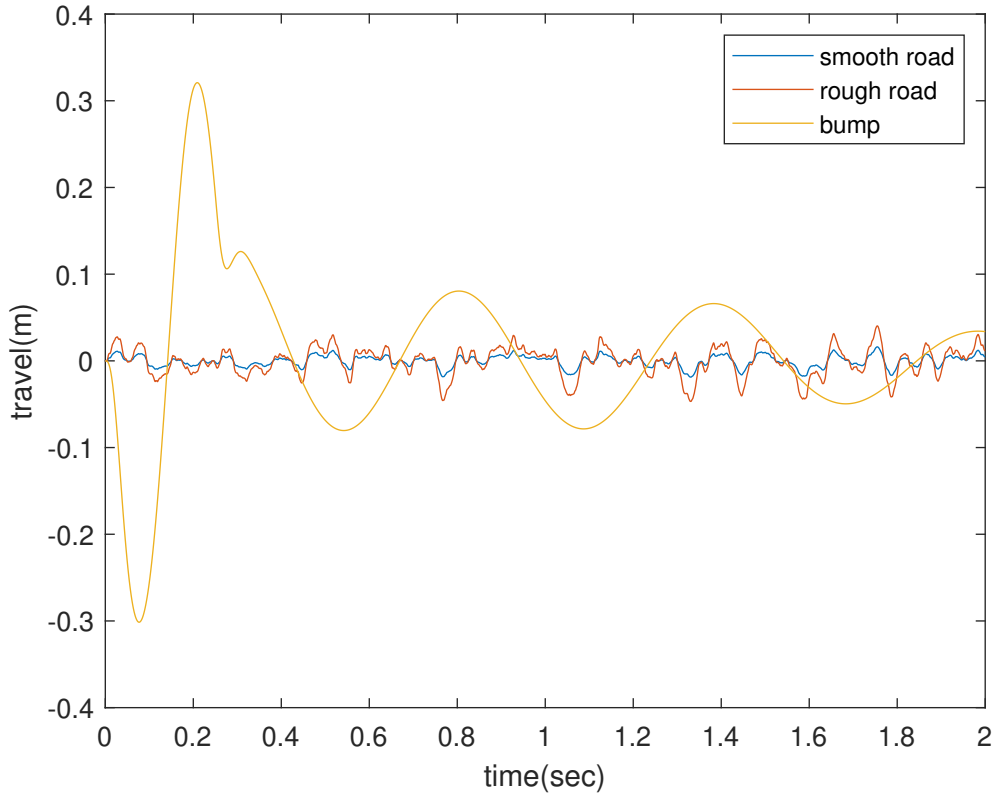

Figure 4.4: Passive suspension system rear suspension travel based on road profiles

	RMS Value $[m]$	PSD maximum amplitude $[dB/Hz]$
smooth road	0.0066	$1.6785x10^{-5}$
rough road	0.0164	$1.0482x10^{-4}$
bump	0.0943	0.0116

Table 4.4: RMS values and PSD maximum amplitudes based on various road conditions for rear suspension travel for passive suspension system

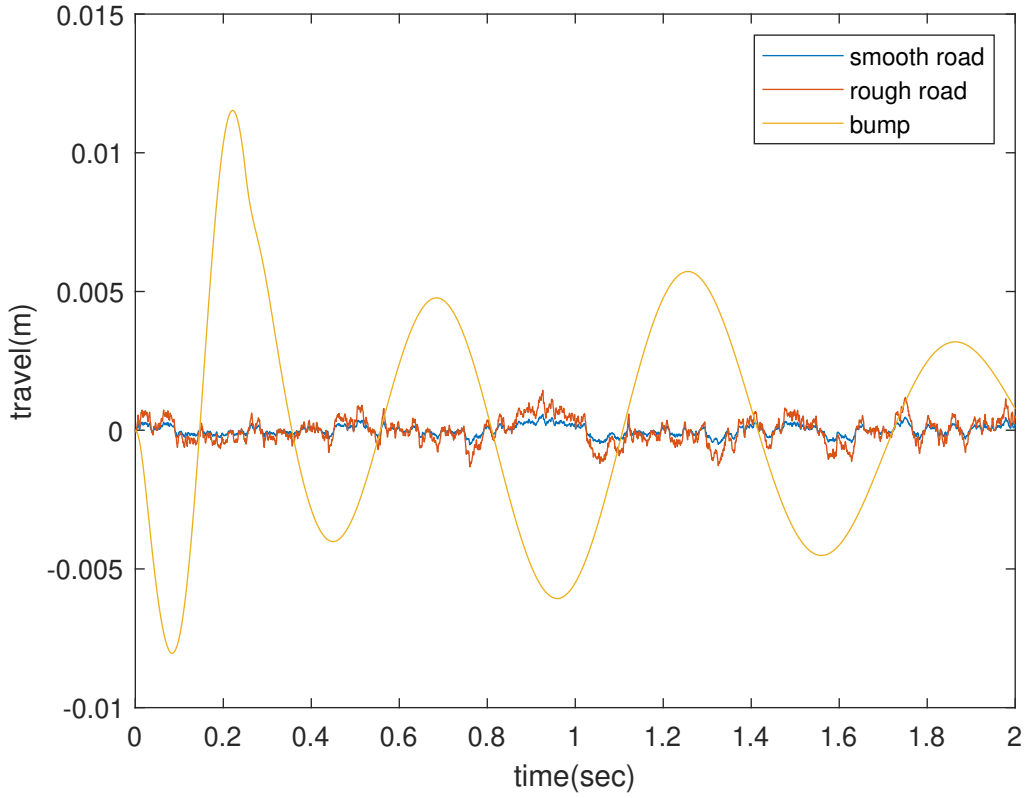

Figure 4.5: Passive suspension system front tire compression based on road profiles

	RMS Value $[m]$	PSD maximum amplitude $[dB/Hz]$
smooth road	$1.8141x10^{-4}$	$2.1820x10^{-8}$
rough road	$4.5362x10^{-4}$	$1.3662x10^{-7}$
bump	0.0042	$3.5299x10^{-5}$

Table 4.5: RMS values and PSD maximum amplitudes based on various road conditions for front tire compression for passive suspension system

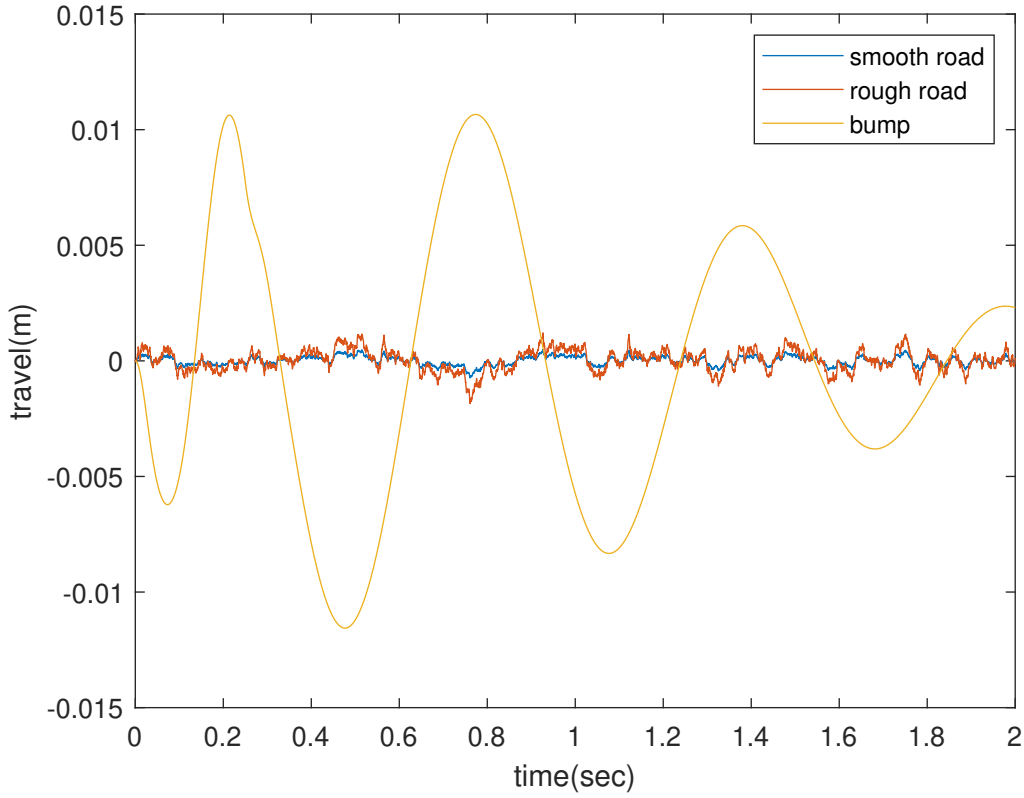

Figure 4.6: Passive suspension system rear tire compression based on road profiles

	RMS Value $[m]$	PSD maximum amplitude $[dB/Hz]$
smooth road	$1.8365x10^{-4}$	$2.2159x10^{-8}$
rough road	$4.5924x10^{-4}$	$1.3865x10^{-7}$
bump	0.0058	$7.0286x10^{-5}$

Table 4.6: RMS values and PSD maximum amplitudes based on various road conditions for rear tire compression for passive suspension system

4.2 H_∞ Control Simulation Results

H_∞ controller design approach attempts to improve the riding comfort of suspension system and handling. In the controller design, the weights described in the preceding section are used. Acceleration, suspension movement, tire compression, and actuator efforts are the data to be employed in the performance evaluation.

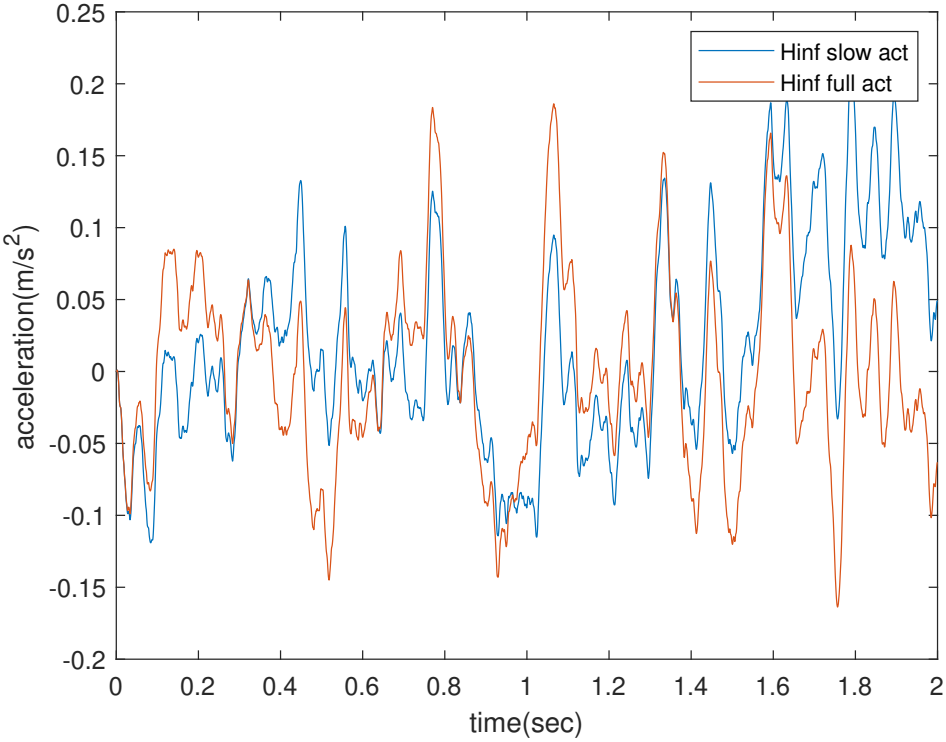

Figure 4.7: H_∞ control linear acceleration on smooth road

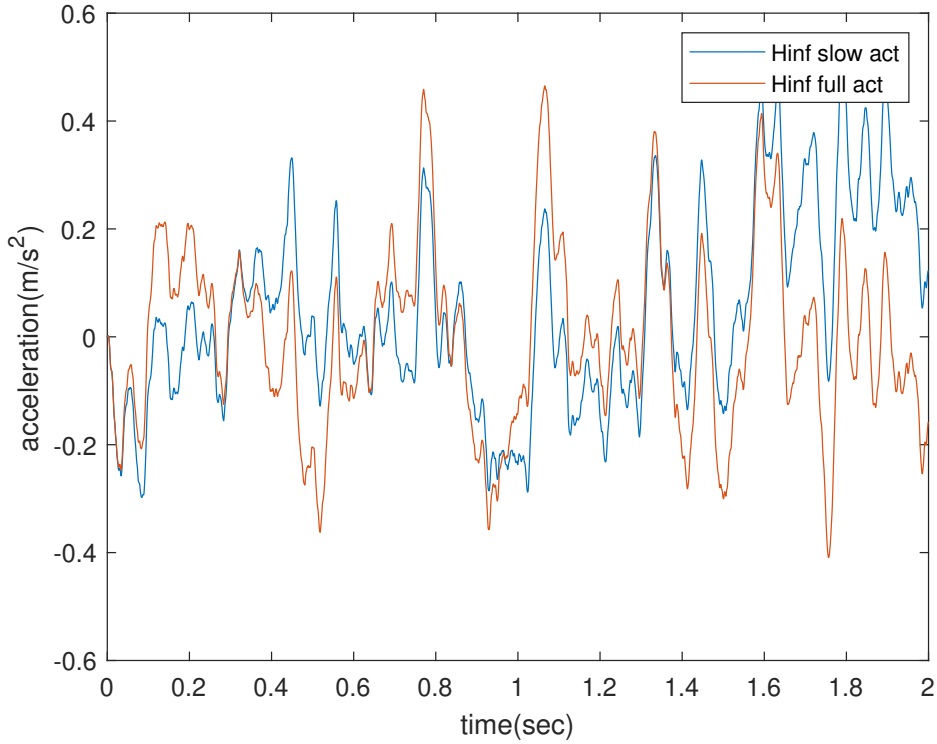

Figure 4.8: H_∞ control linear acceleration on rough road

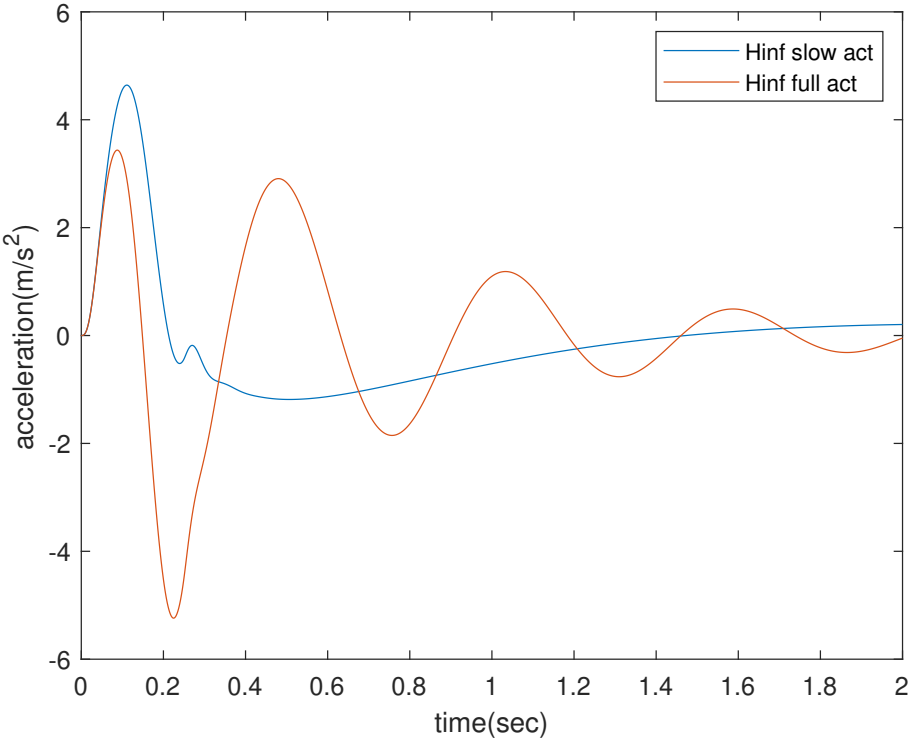

Figure 4.9: H_∞ control linear acceleration on bump

	Slow-active RMS Value $[m/s^2]$	 PSD maximum amplitude $[dB/Hz]$
smooth road	0.0739	0.0041
rough road	0.1848	0.0256
bump	1.6502	4.7051
	Full-active RMS Value $[m/s^2]$	 PSD maximum amplitude $[dB/Hz]$
smooth road	0.0676	0.0035
rough road	0.1691	0.0219
bump	1.5807	4.6565

Table 4.7: RMS values and PSD maximum amplitudes based on various road conditions linear body acceleration for slow-active and full-active suspensions controlled by H_∞ controller

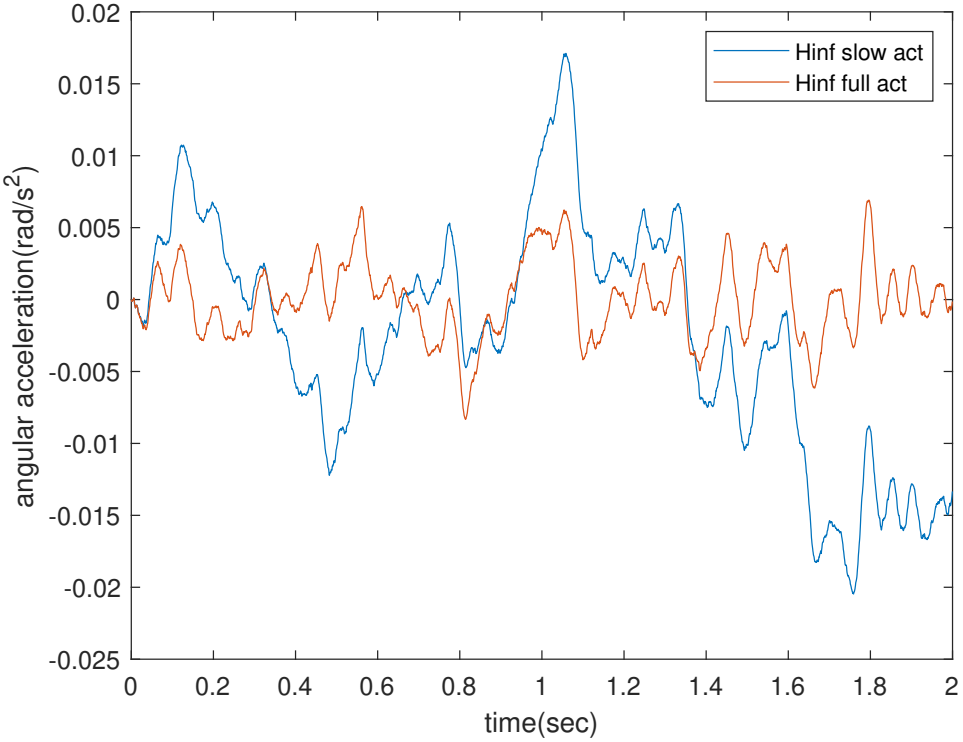

Figure 4.10: H_∞ control angular acceleration on smooth road

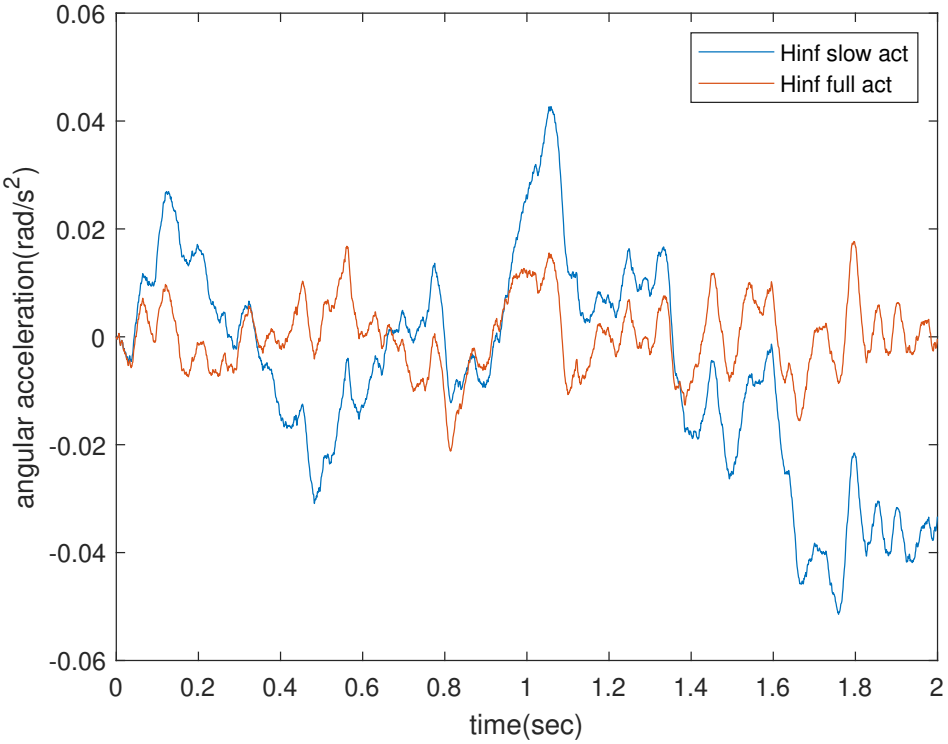

Figure 4.11: H_∞ control angular acceleration on rough road

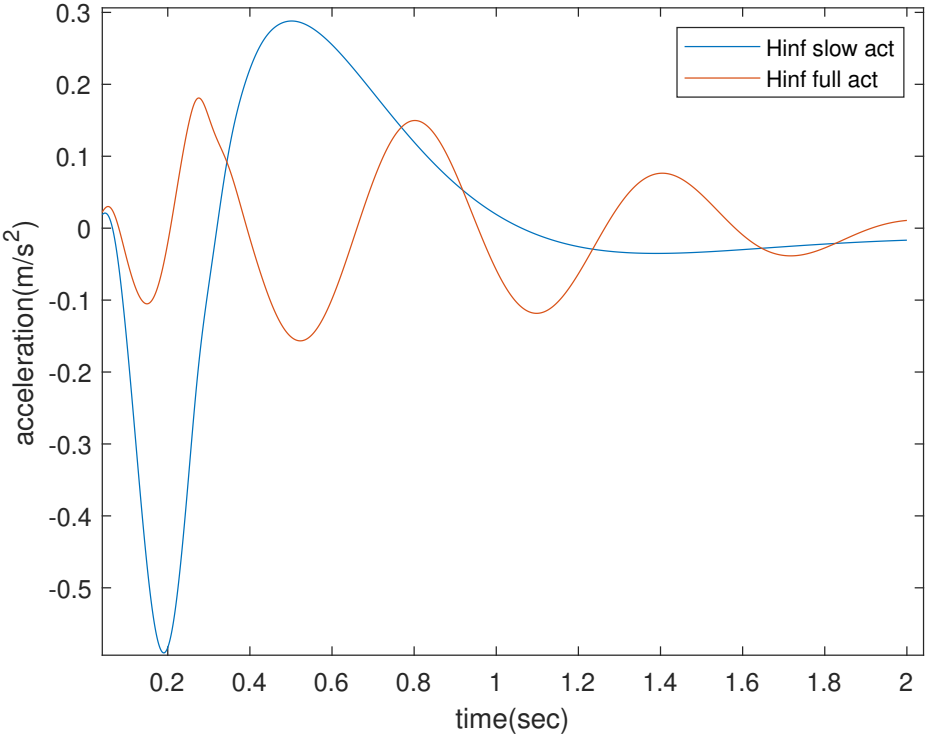

Figure 4.12: H_∞ control angular acceleration on bump

	Slow-active RMS Value $[rad/s^2]$	 PSD maximum amplitude $[dB/Hz]$
smooth road	0.0084	$9.5269x10^{-5}$
rough road	0.0211	$5.59x10^{-4}$
bump	0.1751	0.0369
	Full-active RMS Value $[rad/s^2]$	 PSD maximum amplitude $[dB/Hz]$
smooth road	0.0027	$5.2052x10^{-6}$
rough road	0.0067	$3.2413x10^{-5}$
bump	0.0811	0.0105

Table 4.8: RMS values and PSD maximum amplitudes based on various road conditions angular body acceleration for slow-active and full-active suspensions controlled by H_∞ controller

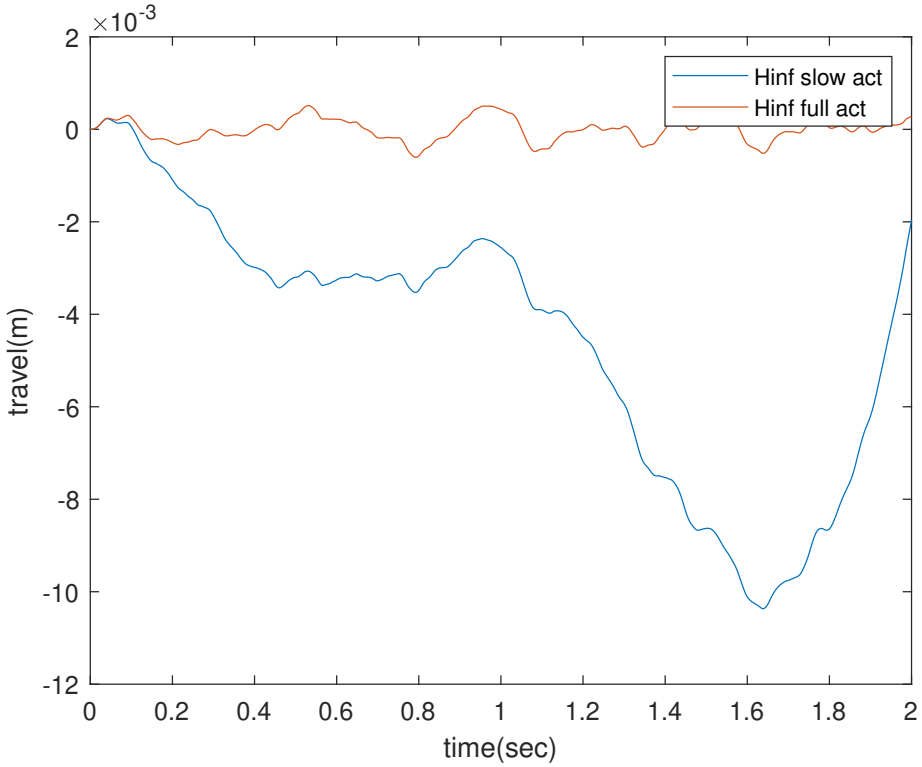

Figure 4.13: H_∞ control front suspension travel on smooth road

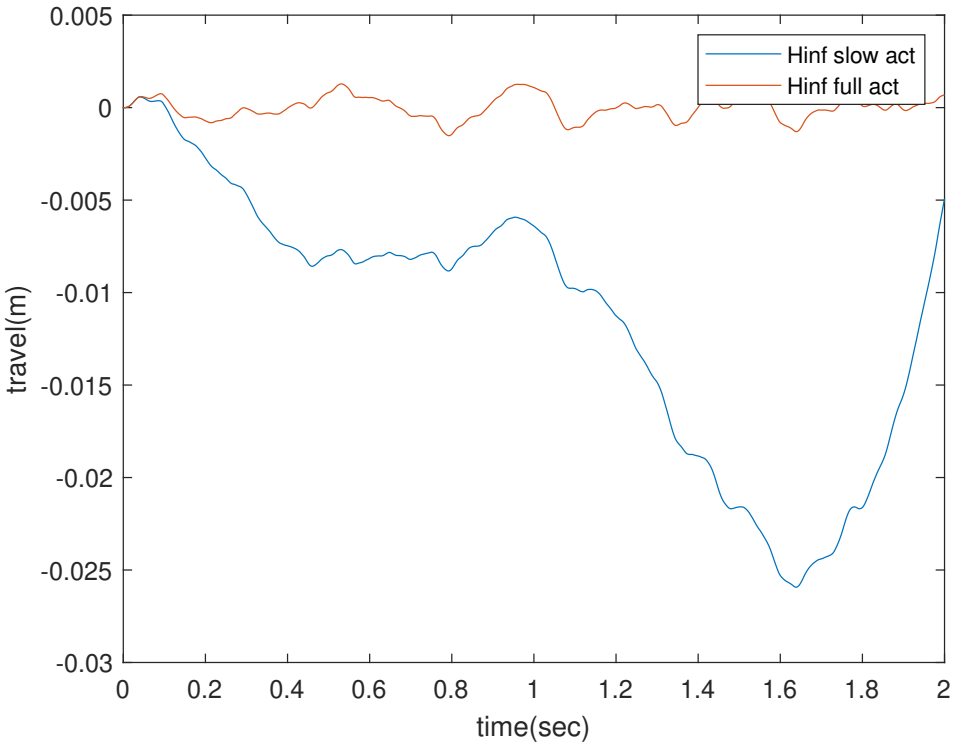

Figure 4.14: H_∞ control front suspension travel on rough road

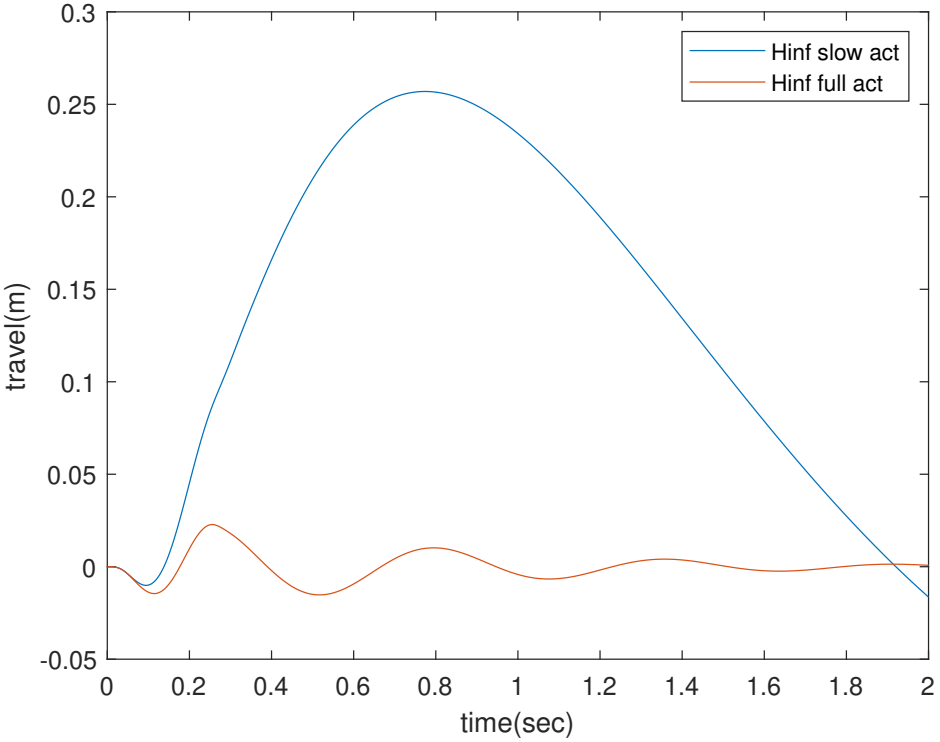

Figure 4.15: H_∞ control front suspension travel on bump

	Slow-active	
	RMS Value $[m]$	PSD maximum amplitude $[dB/Hz]$
smooth road	0.0054	$8.2566x10^{-5}$
rough road	0.0135	$5.1702x10^{-4}$
bump	0.1639	0.0738
	Full-active	
	RMS Value $[m]$	PSD maximum amplitude $[dB/Hz]$
smooth road	$2.4565x10^{-4}$	$7.1425x10^{-8}$
rough road	$6.1432x10^{-4}$	$4.4699x10^{-7}$
bump	0.0078	$1.2035x10^{-4}$

Table 4.9: RMS values and PSD maximum amplitudes based on various road conditions front suspension travel for slow-active and full-active suspensions controlled by H_∞ controller

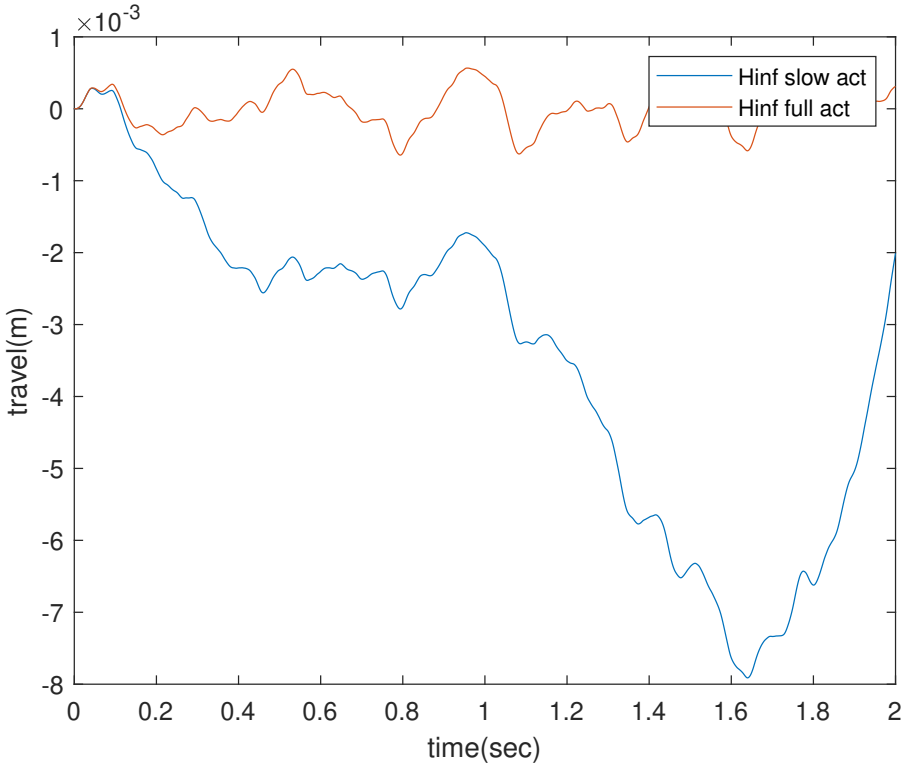

Figure 4.16: H_∞ control rear suspension travel on smooth road

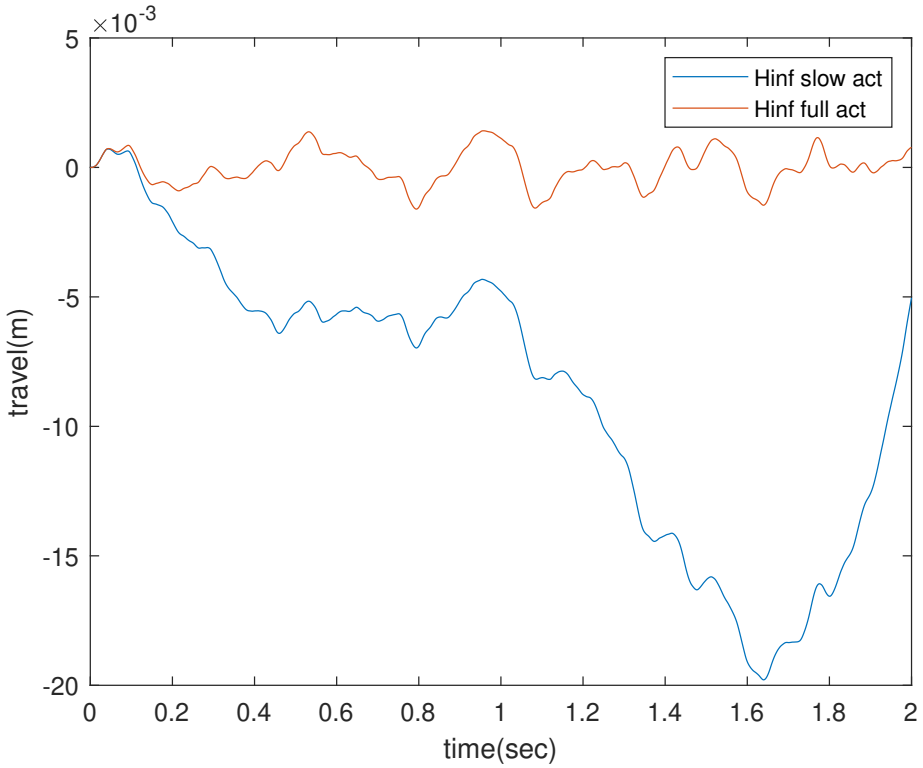

Figure 4.17: H_∞ control rear suspension travel on rough road

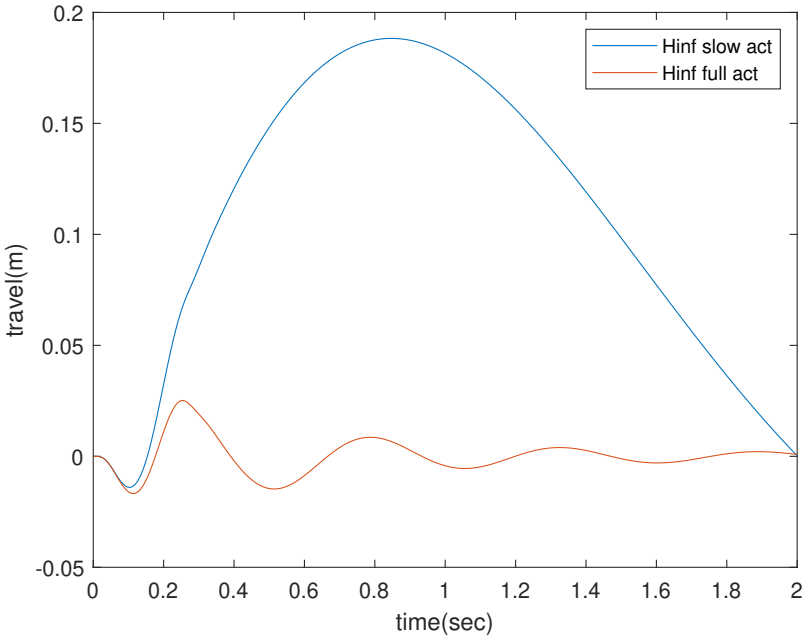

Figure 4.18: H_∞ control rear suspension travel on bump

	Slow-active	
	RMS Value $[m]$	PSD maximum amplitude $[dB/Hz]$
smooth road	0.0041	$4.7453x10^{-5}$
rough road	0.0103	$2.9725x10^{-4}$
bump	0.1259	0.0463
	Full-active	
	RMS Value $[m]$	PSD maximum amplitude $[dB/Hz]$
smooth road	$2.7384x10^{-4}$	$7.7410x10^{-8}$
rough road	$6.8465x10^{-4}$	$4.8399x10^{-7}$
bump	0.0079	$1.2826x10^{-4}$

Table 4.10: RMS values and PSD maximum amplitudes based on various road conditions rear suspension travel for slow-active and full-active suspensions controlled by H_∞ controller

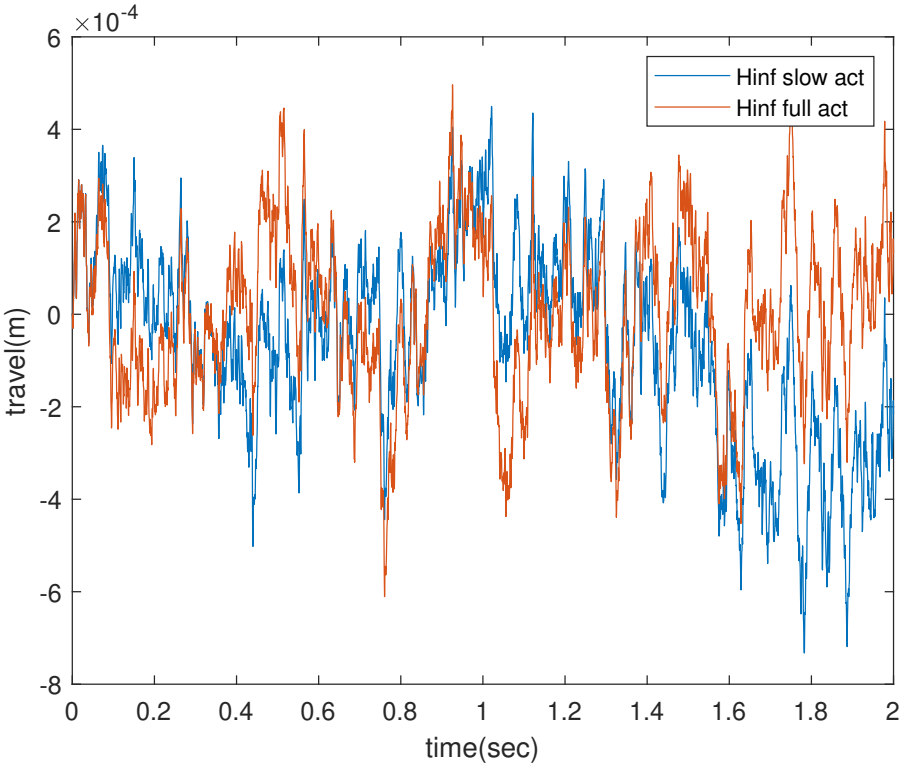

Figure 4.19: H_∞ control front tire compression on smooth road

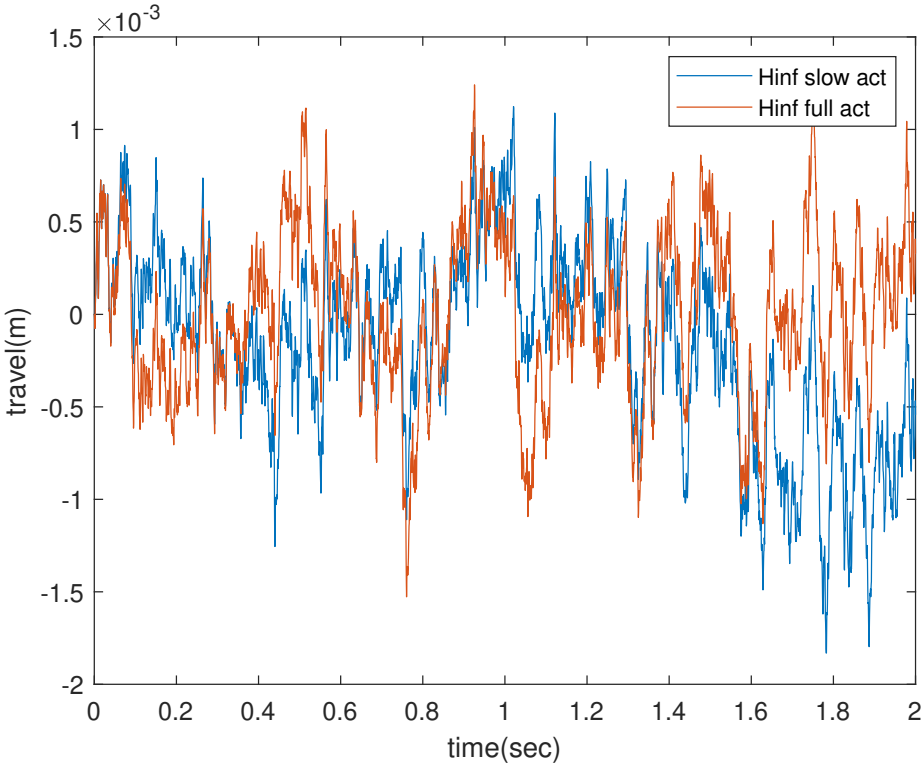

Figure 4.20: H_∞ control front tire compression on rough road

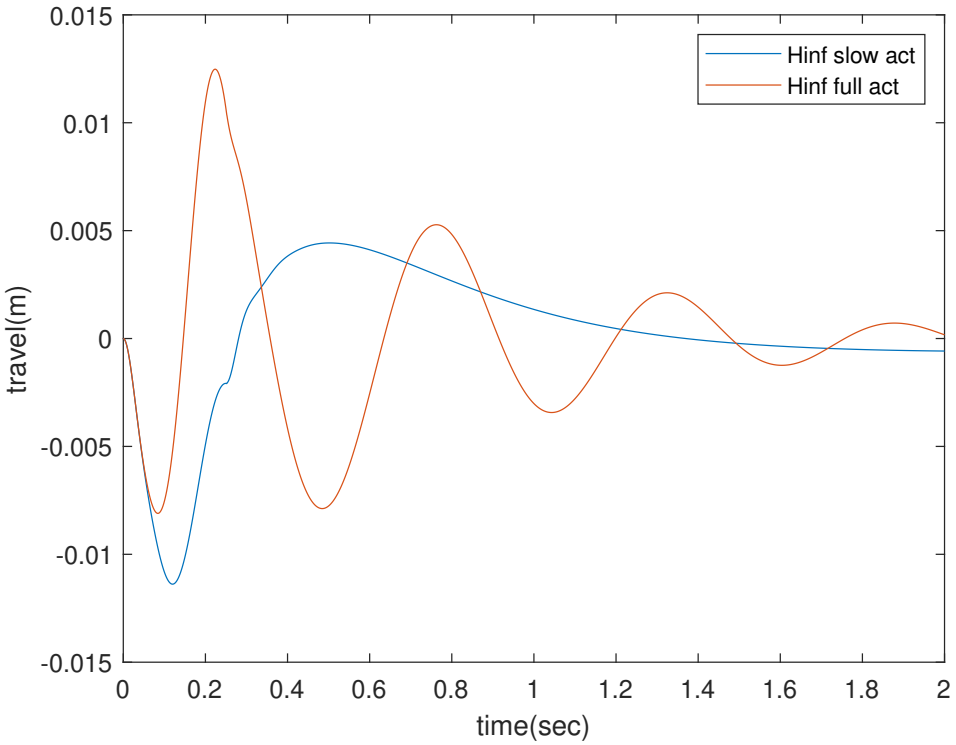

Figure 4.21: H_∞ control front tire compression on bump

	Slow-active	
	RMS Value $[m]$	PSD maximum amplitude $[dB/Hz]$
smooth road	$2.1688x10^{-4}$	$3.9902x10^{-8}$
rough road	$5.4216x10^{-4}$	$2.4944x10^{-7}$
bump	0.0053	$2.6439x10^{-5}$
	Full-active	
	RMS Value $[m]$	PSD maximum amplitude $[dB/Hz]$
smooth road	$1.7709x10^{-4}$	$2.1108x10^{-8}$
rough road	$4.4280x10^{-4}$	$1.3209x10^{-7}$
bump	0.0041	$3.2441x10^{-5}$

Table 4.11: RMS values and PSD maximum amplitudes based on various road conditions front tire compression for slow-active and full-active suspensions controlled by H_∞ controller

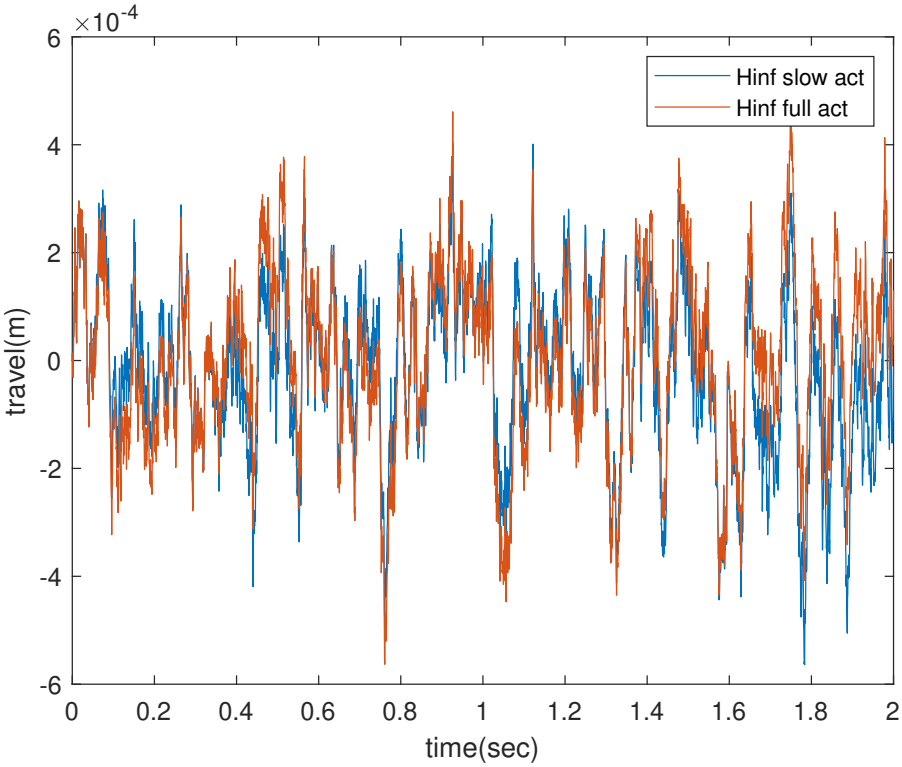

Figure 4.22: H_∞ control rear tire compression on smooth road

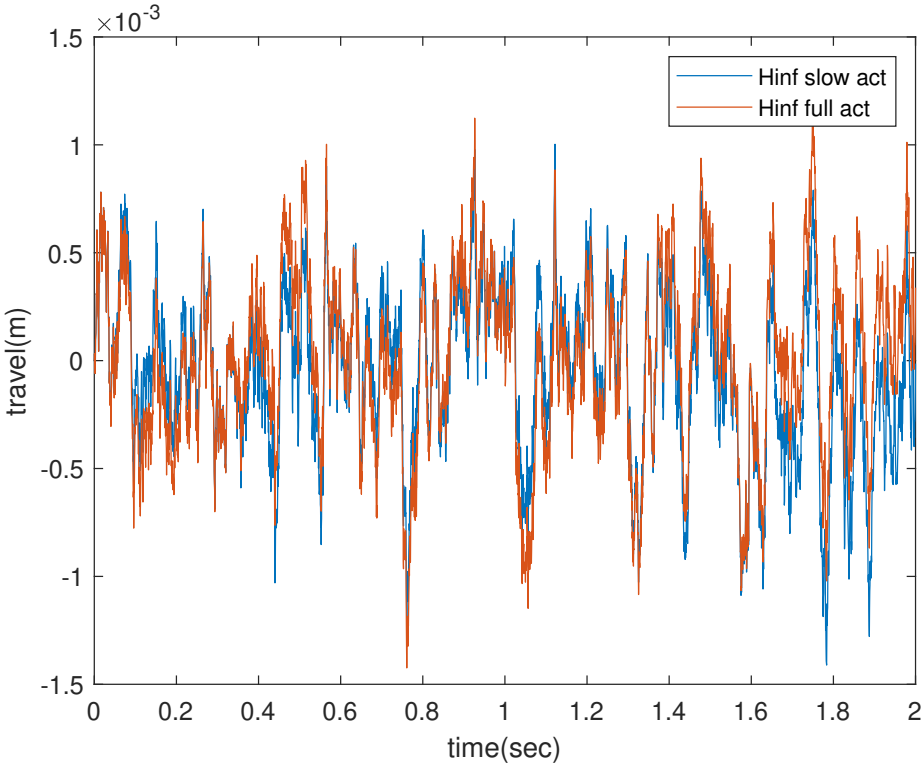

Figure 4.23: H_∞ control rear tire compression on rough road

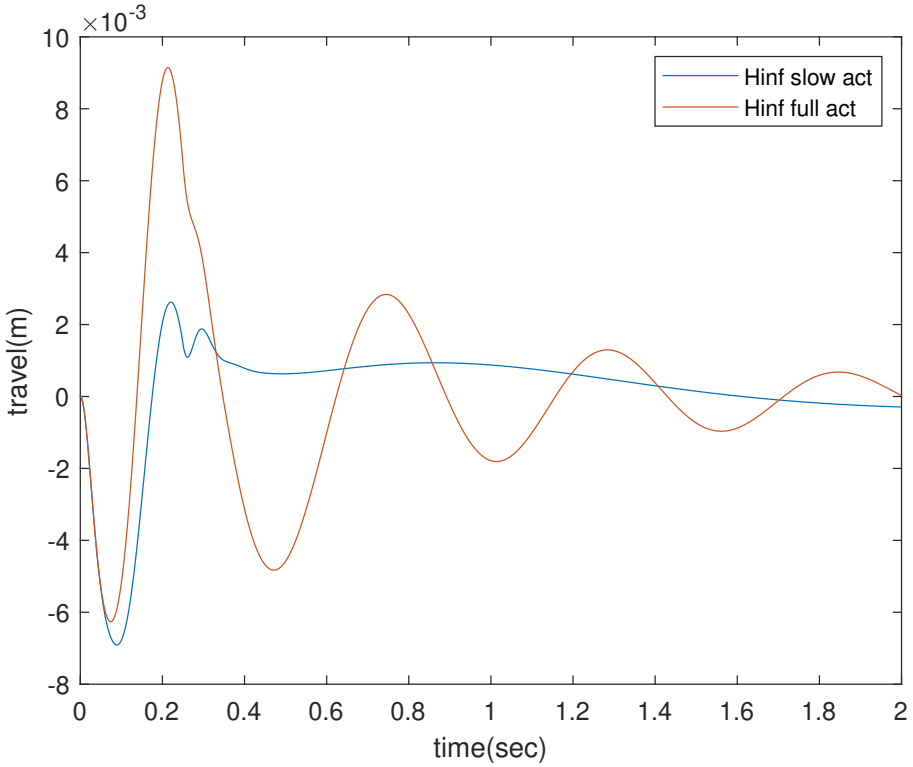

Figure 4.24: H_∞ control rear tire compression on bump

	Slow-active	
	RMS Value $[m]$	PSD maximum amplitude $[dB/Hz]$
smooth road	$1.5497x10^{-4}$	$6.6365x10^{-9}$
rough road	$3.8746x10^{-4}$	$4.1532x10^{-8}$
bump	0.0036	$2.2198x10^{-5}$
	Full-active	
	RMS Value $[m/s^2]$	PSD maximum amplitude $[dB/Hz]$
smooth road	$1.6160x10^{-4}$	$1.1091x10^{-8}$
rough road	$4.04003x10^{-4}$	$6.9329x10^{-8}$
bump	0.0027	$1.3912x10^{-5}$

Table 4.12: RMS values and PSD maximum amplitudes based on various road conditions rear tire compression for slow-active and full-active suspensions controlled by H_∞ controller

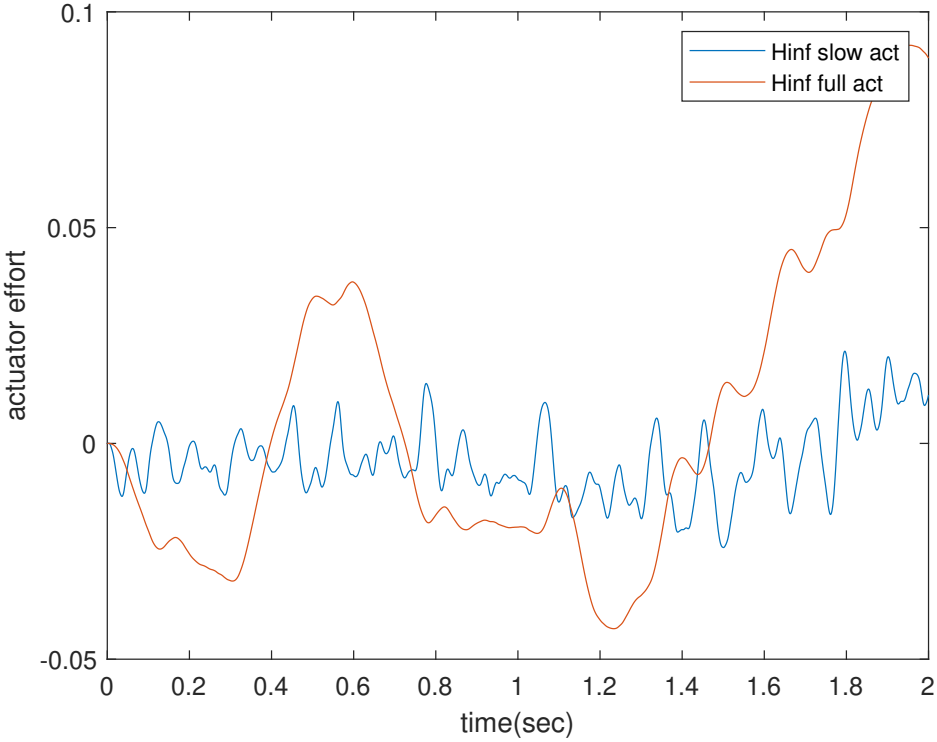

Figure 4.25: H_∞ control front actuator effort on smooth road

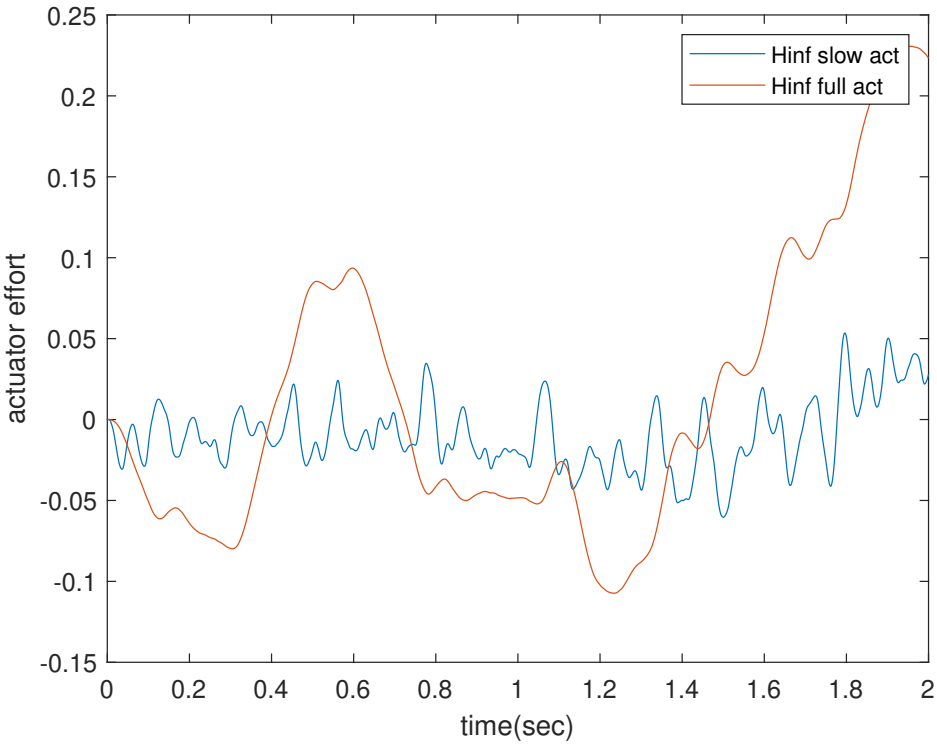

Figure 4.26: H_∞ control front actuator effort on rough road

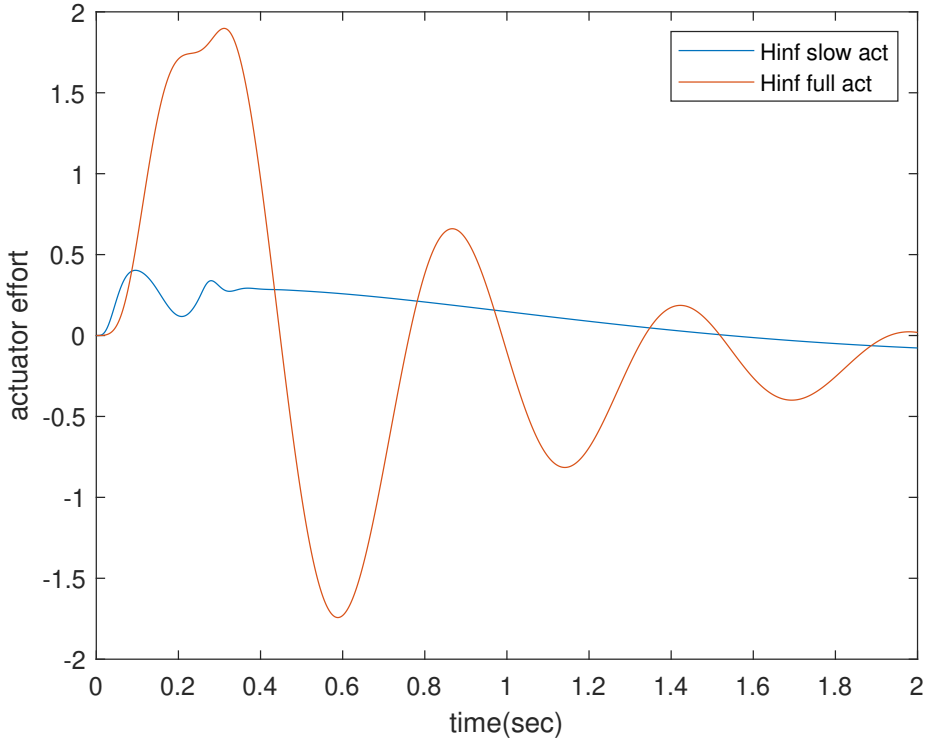

Figure 4.27: H_∞ control front actuator effort on bump

	Slow-active	
	RMS Value	PSD maximum amplitude
smooth road	0.0094	$5.8197x10^{-5}$
rough road	0.0236	$3.6470x10^{-4}$
bump	0.1821	0.0650
	Full-active	
	RMS Value	PSD maximum amplitude
smooth road	0.0360	0.0020
rough road	0.0900	0.0124
bump	0.8470	1.1835

Table 4.13: RMS values and PSD maximum amplitudes based on various road conditions front actuator effort for slow-active and full-active suspensions controlled by H_∞ controller

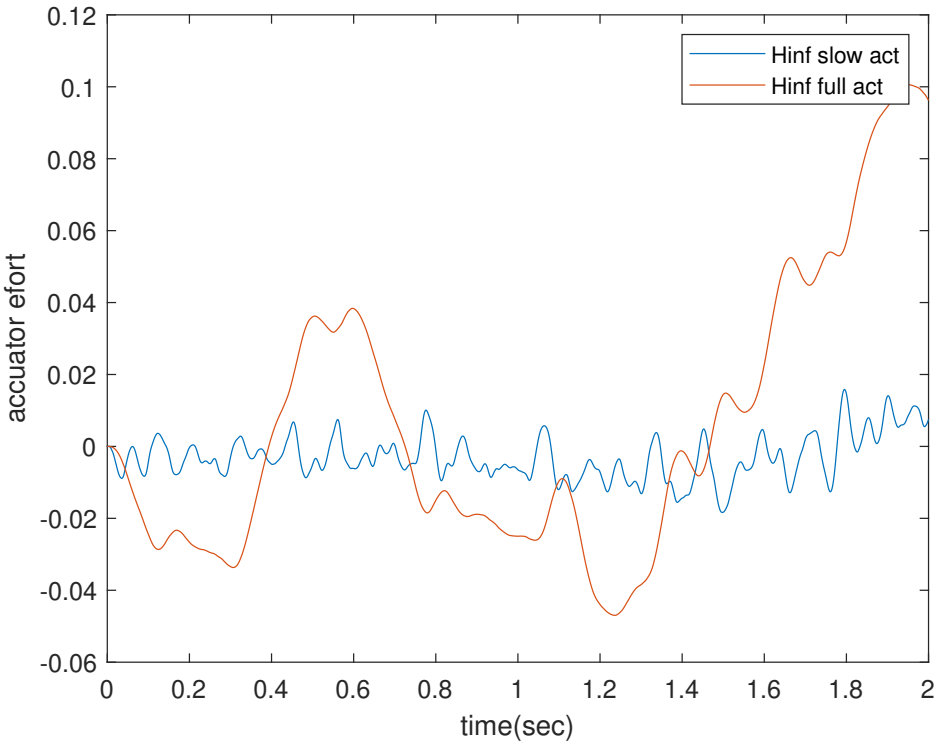

Figure 4.28: H_∞ control rear actuator effort on smooth road

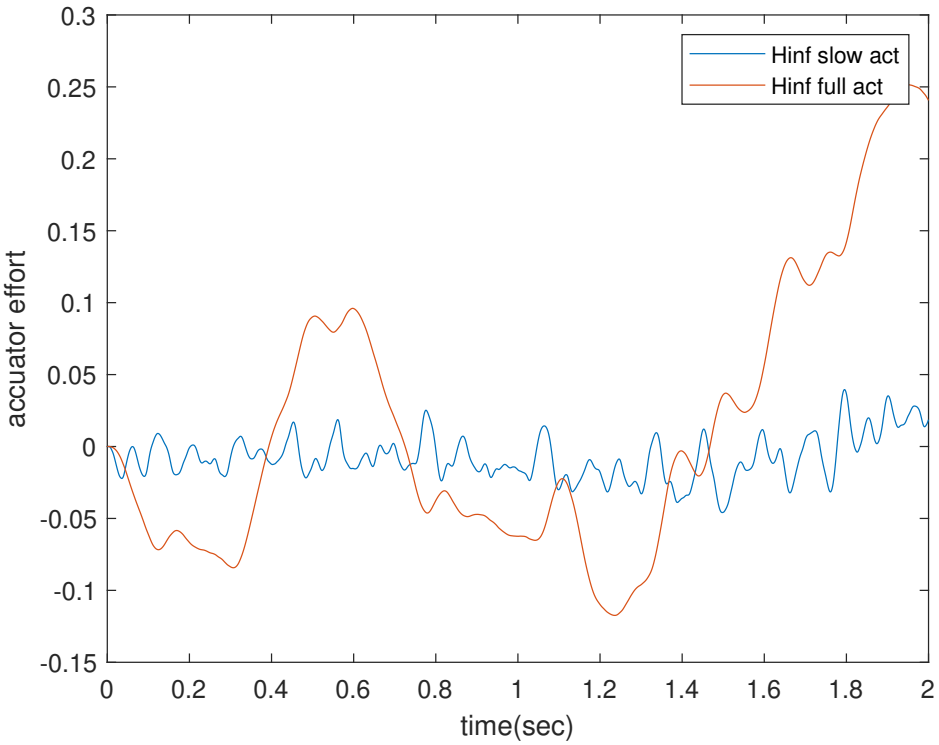

Figure 4.29: H_∞ control rear actuator effort on rough road

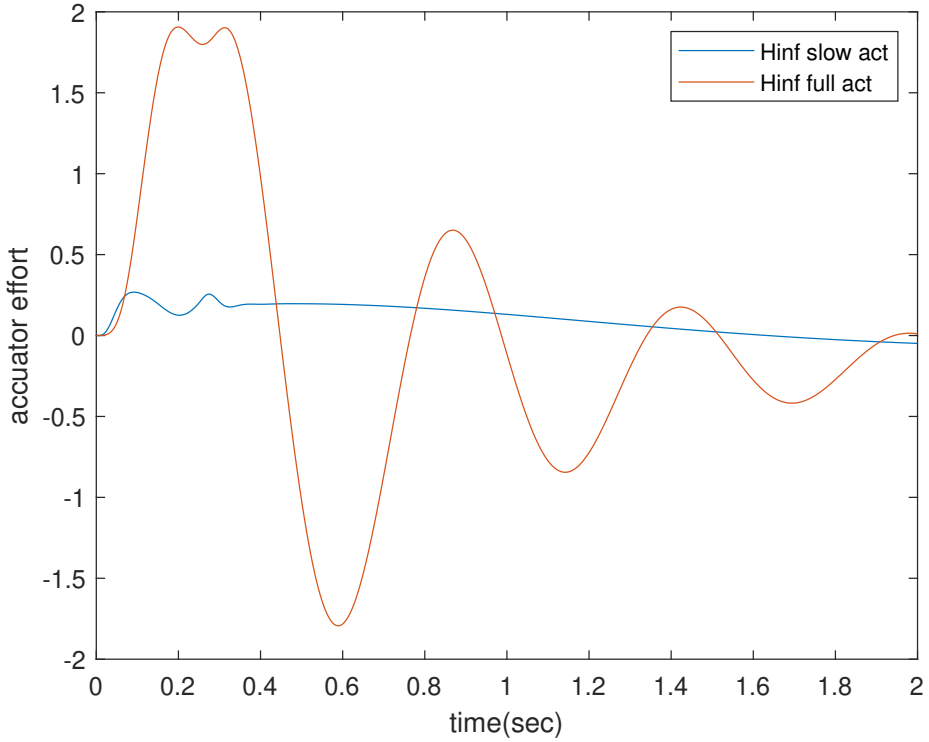

Figure 4.30: H_∞ control rear actuator effort on bump

	Slow-active	
	RMS Value	PSD maximum amplitude
smooth road	0.0069	$3.6967x10^{-5}$
rough road	0.0173	$2.3173x10^{-4}$
bump	0.1366	0.0432
	Full-active	
	RMS Value	PSD maximum amplitude
smooth road	0.0391	0.0023
rough road	0.0977	0.0146
bump	0.8860	1.2934

Table 4.14: RMS values and PSD maximum amplitudes based on various road conditions rear actuator effort for slow-active and full-active suspensions controlled by H_∞ controller

The result of μ-analysis shows H_∞ the controller's slow-active suspension can tolerate an extra 110% of the uncertainty for each parameter. H_∞ the controller's full-active suspension can manage up an extra 194% of the uncertainty for each parameter. The 4.15 table shows the limits of parameters in terms of slow-active and full-active suspension systems.

Table 4.15: Uncertainty rages result of μ-analysis of close-loop suspension systems

		slow-active suspension	full-active suspension
	Mean value	Deviation	
M_b	997 kg	-93.5 +165 kg	-161.5 +291 kg
c_{b_f}	3500 Ns/m	-650 +270 Ns/m	-1067 +485 Ns/m
c_{b_r}	2800 Ns/m	-650 +270 Ns/m	-1067 +485 Ns/m
k_{w_f}	2.34e5 N/m	$\pm$0.33e5 N/m	$\pm$0.582e5 N/m
k_{w_r}	2.34e5 N/m	$\pm$0.33e5 N/m	$\pm$0.582e5 N/m

4.3 Evaluation of Simulations

Two alternative suspension systems outperformed the passive suspension system in simulations. The tables below offer data on riding comfort, handling, and actuator effort for compassion controllers versus passive systems.

The tables below compare the ride comforts of various systems based on linear and angular acceleration. In general, the four systems offer more comfort than the passive suspension system.

	smooth road condition	
	RMS Value Chance [%]	PSD MA Change [%]
Passive	—	—
H_∞ with slow-active	5.49	8.88
H_∞ with full-active	13.55	22.22

Table 4.16: Comparison table of suspensions linear accelerations based on RMS and PSD values on smooth road condition

	rough road condition	
	RMS Value Chance [%]	PSD MA Change [%]
Passive	—	—
H_∞ with slow-active	2.94	19.24
H_∞ with full-active	11.18	30.91

Table 4.17: Comparison table of suspensions linear accelerations based on RMS and PSD values on rough road condition

	bump condition	
	RMS Value Chance [%]	PSD MA Change [%]
Passive	—	—
H_∞ with slow-active	6.94	16.72
H_∞ with full-active	10.86	17.6

Table 4.18: Comparison table of suspensions linear accelerations based on RMS and PSD values on bump condition

Linear accelerations are compared in the tables. 4.16,4.17 and 4.18 show that full-active suspension controlled by H_∞ controller outperforms passive suspension. The slow-active suspension system controlled by H_∞ controller is the second-best system.

	smooth road condition	
	RMS Value Chance [%]	PSD MA Change [%]
Passive	—	—
H_∞ with slow-active	37.31	68.79
H_∞ with full-active	79.85	98.29

Table 4.19: Comparison table of suspensions angular accelerations based on RMS and PSD values on smooth road condition

	rough road condition	
	RMS Value Chance [%]	PSD MA Change [%]
Passive	—	—
H_∞ with slow-active	37.01	68.67
H_∞ with full-active	80	98.29

Table 4.20: Comparison table of suspensions angular accelerations based on RMS and PSD values on rough road condition

	bump condition	
	RMS Value Chance [%]	PSD MA Change [%]
Passive	—	—
H_∞ with slow-active	76.46	97.31
H_∞ with full-active	89.09	99.23

Table 4.21: Comparison table of suspensions angular accelerations based on RMS and PSD values on bump condition

The comparison of angular accelerations 4.19, 4.20 and 4.21 demonstrate that the best performing system is full-active suspension controlled by H_∞ controller. The slow-active suspension system controlled by a H_∞ controller is the second-best solution.

	smooth road condition	
	RMS Value Chance [%]	PSD MA Change [%]
Passive	—	—
H_∞ with slow-active	-1.85	-5.81
H_∞ with full-active	7.22	26.78

Table 4.22: Comparison table of suspensions average tire compression based on RMS and PSD values on smooth road condition

	rough road condition	
	RMS Value Chance [%]	PSD MA Change [%]
Passive	—	—
H_∞ with slow-active	-1.79	-5.70
H_∞ with full-active	7.27	26.82

Table 4.23: Comparison table of suspensions average tire compression based on RMS and PSD values on rough road condition

	bump condition	
	RMS Value Chance [%]	PSD MA Change [%]
Passive	—	—
H_∞ with slow-active	11	53.93
H_∞ with full-active	32	56.09

Table 4.24: Comparison table of suspensions average tire compression based on RMS and PSD values on bump condition

Tables 4.22, 4.23 and 4.24 demonstrates that the best performing system is full-active suspension controlled by H_∞ controller. The worst performed system is the slow-active suspension system controlled by a H_∞ controller.

	smooth road condition	
	RMS Value	PSD maximum amplitude
Passive	—	—
H_∞ with slow-active	$7.9x10^{-3}$	$4.89x10^{-5}$
H_∞ with full-active	$3.76x10^{-2}$	$2.15x10^{-3}$

Table 4.25: Comparison table of suspensions average actuator effort based on RMS and PSD values on smooth road condition

	rough road condition	
	RMS Value	PSD maximum amplitude
Passive	—	—
H_∞ with slow-active	$2.05x10^{-2}$	$2.98x10^{-4}$
H_∞ with full-active	$9.39x10^{-2}$	$1.35x10^{-2}$

Table 4.26: Comparison table of suspensions average actuator effort based on RMS and PSD values on rough road condition

	bump condition	
	RMS Value	PSD maximum amplitude
Passive	—	—
H_∞ with slow-active	0.159	0.0541
H_∞ with full-active	0.867	1.24

Table 4.27: Comparison table of suspensions average actuator effort based on RMS and PSD values on bump condition

Tables 4.25, 4.26 and 4.27 compare the front and rear actuator effort mean values of the system. The slow-active suspension system that is controlled by H_∞ controller has the lowest energy need.

5. CONCLUSION

The main objective of this thesis is to show, while adjusting H_∞ control, how slow-active and full-active suspensions differ on a half-car model. The systems are compared based on desired performance, which includes riding comfort, handling, and system robustness.

H_∞ controller with full-active suspension system produced the best linear acceleration and angular acceleration performance.The handling performance of the slow-active suspension controlled by H_∞ systems deteriorated. The handling performance of full-active suspension systems controlled by H_∞ controller is improved. H_∞ controller with slow-active suspension system required the least amount of actuator effort.

REFERENCES

[1] Delphi magneride semi-active suspension,http://delphi.com, 2010.

[2] E-active body control suspension system: The car that eliminates poor roads,https://group-media.mercedes-benz.com/marsmediasite/en/instance/ko/e-active-body-control-suspension-system-the-car-that-eliminates-poor-roads.xhtml?oid=43615283, 6 2019.

[3] T. P. J. V. der Sande. Control of an automotive electromagnetic suspension system. Master's thesis, 4 2011.

[4] M. ElMadany, B. A. Bassam, and A. Fayed. Preview control of slow-active suspension systems. *Journal of Vibration and Control*, 17:245–258, 2 2011.

[5] B. L. J. Gysen, J. L. G. Janssen, J. J. H. Paulides, and E. A. Lomonova. Design aspects of an active electromagnetic suspension system for automotive applications. *2008 IEEE Industry Applications Society Annual Meeting*, pages 1–8, 2008.

[6] H. A. Hamersma and S. Els. Comparison of quarter, half and full a vehicle models with experimental ride comfort data. 8 2015.

[7] S. G. Kabil. Alternative control strategies for an electromechanical active suspension system. Master's thesis, 1 2012.

[8] G. P. A. Koch. *Adaptive Control of Mechatronic Vehicle Suspension Systems*. PhD thesis, 2010.

[9] H. Liu, H. Gao, and P. Li, editors. *Handbook of Vehicle Suspension Control Systems*. Institution of Engineering and Technology, 11 2013.

[10] MatWorks. Robust control of an active suspension, https://www.mathworks.com/help/robust/gs/active-suspension-control-design.html.

[11] P. Michelberger, L. Palkovics, and J. Bokor. Robust design of active suspension system. *International Journal of Vehicle Design*, 14:145–165, 1993.

[12] H. B. PACEJKA and I. J. M. BESSELINK. Magic formula tyre model with transient properties. *Vehicle System Dynamics*, 27:234–249, 1997.

[13] A. Soyiçi. Multiobjective output feedback control via lmi optimization and quarter-car active suspension system. Master's thesis, 2009.

[14] P. J. Venhovens. *Optimal Control Of Vehicle Suspensions*. PhD thesis, 11 1993.

[15] C. Vyse. The hydraulic system of the citroën ds explained, 4 2003.

[16] L. Zuo and S. A. Nayfeh. Low order continuous-time filters for approximation of the iso 2631-1 human vibration sensitivity weightings. *Journal of Sound and Vibration*, 265:459–465, 2003.

6. APPENDIX

6.1 Slow-active Half Car Suspension State-space Equation

$$P_{SLA}: \begin{cases} \ddot{x} &= Ax + B_1 w + B_2 u \\ z &= C_1 x + D_{11} w + D_{12} u \\ y &= C_2 x + D_{21} w + D_{22} u \end{cases} \qquad P_{SLA}(s): \left[\begin{array}{c|cc} A & B_1 & B_2 \\ \hline C_1 & D_{11} & D_{12} \\ C_2 & D_{21} & D_{22} \end{array}\right] \tag{6.1}$$

$$A = \begin{bmatrix}
0 & 1 & 0 & 0 & 0 & 0 & 0 & 0 & 0 & 0 & 0 & 0 \\
0 & \frac{-{l_f}^2 c_{b_f} - {l_r}^2 c_{b_r}}{J_y} & 0 & \frac{-l_f c_{b_f} + l_r c_{b_r}}{J_y} & \frac{l_f k_{b_f}}{J_y} & \frac{l_f c_{b_f}}{J_y} & \frac{-l_r k_{b_r}}{J_y} & \frac{-l_r c_{b_r}}{J_y} & \frac{-l_f k_{b_f}}{J_y} & 0 & \frac{l_r k_{b_r}}{J_y} & 0 \\
0 & 0 & 0 & 1 & 0 & 0 & 0 & 0 & 0 & 0 & 0 & 0 \\
0 & \frac{-l_f c_{b_f} + l_r c_{b_r}}{M_b} & 0 & \frac{-c_{b_f} - c_{b_r}}{M_b} & \frac{k_{b_f}}{M_b} & \frac{c_{b_f}}{M_b} & \frac{k_{b_r}}{M_b} & \frac{c_{b_r}}{M_b} & \frac{-k_{b_f}}{M_b} & 0 & \frac{-k_{b_r}}{M_b} & 0 \\
0 & 0 & 0 & 0 & 1 & 0 & 0 & 0 & 0 & 0 & 0 & 0 \\
0 & \frac{-l_f c_{b_f}}{m_{w_r}} & 0 & \frac{c_{b_f}}{m_{w_f}} & \frac{-k_{b_f} - k_{w_f}}{m_{w_f}} & \frac{-c_{b_f}}{m_{w_f}} & 0 & 0 & \frac{k_{b_f}}{m_{w_f}} & 0 & 0 & 0 \\
0 & 0 & 0 & 0 & 0 & 0 & 1 & 0 & 0 & 0 & 0 & 0 \\
0 & \frac{-l_r c_{b_r}}{m_{w_r}} & 0 & \frac{c_{b_r}}{m_{w_r}} & 0 & 0 & \frac{-k_{b_r} - k_{w_r}}{m_{w_r}} & \frac{-c_{b_r}}{m_{w_r}} & 0 & 0 & \frac{k_{b_r}}{m_{w_r}} & 0 \\
0 & 0 & 0 & 0 & 0 & 0 & 0 & 0 & 0 & 1 & 0 & 0 \\
{l_f w_{0,\mathrm{act}_f}}^2 & 2 l_f \zeta_f w_{0,\mathrm{act}_f} - l_f c_{b_f} a_1 + l_r c_{b_r} a_2 & {w_{0,\mathrm{act}_f}}^2 & 2\zeta_f w_{0,\mathrm{act}_f} - c_{b_f} a_1 - c_{b_r} a_2 & k_{b_f} a_1 & c_{b_f} a_1 & k_{b_r} a_2 & c_{b_r} a_2 & -{w_{0,\mathrm{act}_f}}^2 - k_{b_f} a_1 & -2\zeta_f w_{0,\mathrm{act}_f} & -k_{b_f} a_2 & 0 \\
0 & 0 & 0 & 0 & 0 & 0 & 0 & 0 & 0 & 0 & 0 & 1 \\
-l_r {w_{0,\mathrm{act}_r}}^2 & -2 l_r \zeta_r w_{0,\mathrm{act}_r} - l_f c_{b_f} a_2 + l_r c_{b_r} a_3 & {w_{0,\mathrm{act}_r}}^2 & 2\zeta_r w_{0,\mathrm{act}_r} - c_{b_f} a_2 - c_{b_r} a_3 & k_{b_f} a_2 & c_{b_f} a_2 & k_{b_r} a_3 & c_{b_r} a_3 & -k_{b_f} a_2 & 0 & -{w_{0,\mathrm{act}_r}}^2 - k_{b_r} a_3 & -2\zeta_r w_{0,\mathrm{act}_r}
\end{bmatrix}$$

$$z_s = [\theta \quad \dot{\theta} \quad z_b \quad \dot{z}_b \quad z_{w_f} \quad \dot{z}_{w_f} \quad z_{w_r} \quad \dot{z}_{w_r} \quad z_{act,f} \quad \dot{z}_{act,r} \quad z_{act,r} \quad \dot{z}_{act,r}]^T \tag{6.2}$$

$$B_1 = \begin{bmatrix} 0 & 0 \\ 0 & 0 \\ 0 & 0 \\ 0 & 0 \\ 0 & 0 \\ \frac{k_{w_f}}{m_{w_f}} & 0 \\ 0 & 0 \\ 0 & \frac{k_{w_r}}{m_{w_r}} \\ 0 & 0 \\ 0 & 0 \\ 0 & 0 \\ 0 & 0 \end{bmatrix} \qquad B_2 = \begin{bmatrix} 0 & 0 \\ 0 & 0 \\ 0 & 0 \\ 0 & 0 \\ 0 & 0 \\ 0 & 0 \\ 0 & 0 \\ 0 & 0 \\ 0 & 0 \\ -w_{0,\mathrm{act}_f}^2 & 0 \\ 0 & 0 \\ 0 & -w_{0,\mathrm{act}_r}^2 \end{bmatrix}$$

$$u_i = [u_f \quad u_r]^T \tag{6.3}$$

$$w_i = [h_f \quad h_r]^T \tag{6.4}$$

$$C_1=\begin{bmatrix} 0 & 0 & 0 & 0 & 1 & 0 & 0 & 0 & 0 & 0 & 0 & 0 \\ 0 & 0 & 0 & 0 & 0 & 0 & 1 & 0 & 0 & 0 & 0 & 0 \\ 0 & \frac{-l_f c_{b_f}+l_r c_{b_r}}{M_b} & 0 & \frac{-c_{b_f}-c_{b_r}}{M_b} & \frac{k_{b_f}}{M_b} & \frac{c_{b_f}}{M_b} & \frac{k_{b_r}}{M_b} & \frac{c_{b_r}}{M_b} & \frac{-k_{b_f}}{M_b} & 0 & \frac{-k_{b_r}}{M_b} & 0 \\ 0 & \frac{-l_f{}^2 c_{b_f}-l_r{}^2 c_{b_r}}{J_y} & 0 & \frac{-l_f c_{b_f}+l_r c_{b_r}}{J_y} & \frac{l_f k_{b_f}}{J_y} & \frac{l_f c_{b_f}}{J_y} & \frac{-l_r k_{b_r}}{J_y} & \frac{-l_r c_{b_r}}{J_y} & \frac{-l_f k_{b_f}}{J_y} & 0 & \frac{l_r k_{b_r}}{J_y} & 0 \\ l_f & 0 & 1 & 0 & -1 & 0 & 0 & 0 & 0 & 0 & 0 & 0 \\ -l_r & 0 & 1 & 0 & 0 & 0 & -1 & 0 & 0 & 0 & 0 & 0 \\ 0 & 0 & 0 & 0 & 0 & 0 & 0 & 0 & 0 & 0 & 0 & 0 \\ 0 & 0 & 0 & 0 & 0 & 0 & 0 & 0 & 0 & 0 & 0 & 0 \end{bmatrix}$$

$$z_o=\begin{bmatrix} z_{w_f}-h_f & z_{w_r}-h_r & \ddot{z}_b & \ddot{\theta} & z_{b_f}-z_{w_f} & z_{b_r}-z_{w_r} & u_f & u_r \end{bmatrix} \tag{6.5}$$

$$C_2=\begin{bmatrix} 0 & \frac{-l_f c_{b_f}+l_r c_{b_r}}{M_b} & 0 & \frac{-c_{b_f}-c_{b_r}}{M_b} & \frac{k_{b_f}}{M_b} & \frac{c_{b_f}}{M_b} & \frac{k_{b_r}}{M_b} & \frac{c_{b_r}}{M_b} & \frac{-k_{b_f}}{M_b} & 0 & \frac{-k_{b_r}}{M_b} & 0 \\ 0 & \frac{-l_f{}^2 c_{b_f}-l_r{}^2 c_{b_r}}{J_y} & 0 & \frac{-l_f c_{b_f}+l_r c_{b_r}}{J_y} & \frac{l_f k_{b_f}}{J_y} & \frac{l_f c_{b_f}}{J_y} & \frac{-l_r k_{b_r}}{J_y} & \frac{-l_r c_{b_r}}{J_y} & \frac{-l_f k_{b_f}}{J_y} & 0 & \frac{l_r k_{b_r}}{J_y} & 0 \\ 0 & \frac{-l_f c_{b_f}}{m_{w_r}} & 0 & \frac{c_{b_f}}{m_{w_f}} & \frac{-k_{b_f}-k_{w_f}}{m_{w_f}} & \frac{-c_{b_f}}{m_{w_f}} & 0 & 0 & \frac{k_{b_f}}{m_{w_f}} & 0 & 0 & 0 \\ 0 & \frac{-l_r c_{b_r}}{m_{w_r}} & 0 & \frac{c_{b_r}}{m_{w_r}} & 0 & 0 & \frac{-k_{b_r}-k_{w_r}}{m_{w_r}} & \frac{-c_{b_r}}{m_{w_r}} & 0 & 0 & \frac{k_{b_r}}{m_{w_r}} & 0 \\ l_f & 0 & 1 & 0 & -1 & 0 & 0 & 0 & 0 & 0 & 0 & 0 \\ -l_r & 0 & 1 & 0 & 0 & 0 & -1 & 0 & 0 & 0 & 0 & 0 \\ 0 & 1 & 0 & 0 & 0 & 0 & 0 & 0 & 0 & 0 & 0 & 0 \end{bmatrix}$$

$$z_o=\begin{bmatrix} \ddot{z}_b & \ddot{\theta} & \ddot{z}_{w_f} & \ddot{z}_{w_r} & z_{b_f}-z_{w_f} & z_{b_r}-z_{w_r} & \dot{\theta} \end{bmatrix} \tag{6.6}$$

$$D_{11}=\begin{bmatrix} -1 & 0 \\ 0 & -1 \\ 0 & 0 \\ 0 & 0 \\ 0 & 0 \\ 0 & 0 \\ 0 & 0 \\ 0 & 0 \end{bmatrix} \quad D_{12}=\begin{bmatrix} 0 & 0 \\ 0 & 0 \\ 0 & 0 \\ 0 & 0 \\ 0 & 0 \\ 0 & 0 \\ 1 & 0 \\ 0 & 1 \end{bmatrix} \quad D_{21}=\begin{bmatrix} 0 & 0 \\ 0 & 0 \\ \frac{k_{wf}}{m_{wf}} & 0 \\ 0 & \frac{k_{wr}}{m_{wr}} \\ 0 & 0 \\ 0 & 0 \\ 0 & 0 \end{bmatrix} \quad D_{22}=\begin{bmatrix} 0 & 0 \\ 0 & 0 \\ 0 & 0 \\ 0 & 0 \\ 0 & 0 \\ 0 & 0 \\ 0 & 0 \\ 0 & 0 \end{bmatrix}$$

6.2 Full-active Half Car Suspension State-space Equation

$$P_{FA}: \begin{cases} \ddot{x} &= Ax + B_1 w + B_2 u \\ z &= C_1 x + D_{11} w + D_{12} u \\ y &= C_2 x + D_{21} w + D_{22} u \end{cases} \qquad P_{FA}(s): \left[\begin{array}{c|cc} A & B_1 & B_2 \\ \hline C_1 & D_{11} & D_{12} \\ C_2 & D_{21} & D_{22} \end{array}\right] \tag{6.7}$$

$$A = \begin{bmatrix} 0 & 1 & 0 & 0 & 0 & 0 & 0 & 0 \\ 0 & \frac{-c_{b_f}-c_{b_r}}{M_b} & 0 & \frac{l_f c_{b_f}-l_r c_{b_r}}{M_b} & \frac{-k_{b_f}}{m_b} & \frac{c_{b_f}}{M_b} & \frac{-k_{b_r}}{M_b} & \frac{c_{b_r}}{M_b} \\ 0 & 0 & 0 & 1 & 0 & 0 & 0 & 0 \\ 0 & \frac{l_f c_{b_f}-l_r c_{b_r}}{J_y} & 0 & \frac{-l_f^2 c_{b_f}-l_r^2 c_{b_r}}{J_y} & \frac{l_f k_{b_f}}{J_y} & \frac{-l_f c_{b_f}}{J_y} & \frac{-l_r k_{b_r}}{J_y} & \frac{l_r c_{b_r}}{J_y} \\ 0 & 1 & 0 & -l_f & 0 & -1 & 0 & 0 \\ \frac{-k_{w_f}}{m_{w_f}} & \frac{c_{b_f}}{m_{w_f}} & \frac{l_f k_{w_f}}{m_{w_f}} & \frac{-l_f c_{b_f}}{m_{w_f}} & \frac{k_{b_f}+k_{w_f}}{m_{w_f}} & \frac{-c_{b_f}}{m_{w_f}} & 0 & 0 \\ 0 & 1 & 0 & l_r & 0 & 0 & 0 & -1 \\ \frac{-k_{w_r}}{m_{w_r}} & \frac{c_{b_r}}{m_{w_r}} & \frac{-l_r k_{w_r}}{m_{w_r}} & \frac{l_r c_{b_r}}{m_{w_r}} & 0 & 0 & \frac{k_{b_r}+k_{w_r}}{m_{w_r}} & \frac{-c_{b_r}}{m_{w_r}} \end{bmatrix}$$

$$z_s = [z_b \quad \dot{z}_b \quad \theta \quad \dot{\theta} \quad z_{b_f} - z_{w_f} \quad \dot{z}_{w_f} \quad z_{b_r} - z_{w_r} \quad \dot{z}_{w_r}]^T \tag{6.8}$$

$$B_1 = \begin{bmatrix} 0 & 0 \\ 0 & 0 \\ 0 & 0 \\ 0 & 0 \\ 0 & 0 \\ \frac{k_{w_f}}{m_{w_f}} & 0 \\ 0 & 0 \\ 0 & \frac{k_{w_r}}{m_{w_r}} \end{bmatrix} \qquad B_2 = \begin{bmatrix} 0 & 0 \\ \frac{1}{M_b} & \frac{1}{M_b} \\ 0 & 0 \\ \frac{-l_f}{J_y} & \frac{l_r}{J_y} \\ 0 & 0 \\ \frac{-1}{m_{w_f}} & 0 \\ 0 & 0 \\ 0 & \frac{-1}{m_{w_r}} \end{bmatrix}$$

$$u_i = [u_f \quad u_r]^T \tag{6.9}$$

$$w_i = [h_f \quad h_r]^T \tag{6.10}$$

$$C_1=\begin{bmatrix} 1 & 0 & -l_f & 0 & -1 & 0 & 0 & 0 \\ 1 & 0 & l_r & 0 & 0 & 0 & -1 & 0 \\ 0 & \frac{-c_{b_f}-c_{b_r}}{M_b} & 0 & \frac{l_f c_{b_f}-l_r c_{b_r}}{M_b} & \frac{-k_{b_f}}{m_b} & \frac{c_{b_f}}{M_b} & \frac{-k_{b_r}}{M_b} & \frac{c_{b_r}}{M_b} \\ 0 & \frac{l_f c_{b_f}-l_r c_{b_r}}{J_y} & 0 & \frac{-l_f^2 c_{b_f}-l_r^2 c_{b_r}}{J_y} & \frac{l_f k_{b_f}}{J_y} & \frac{-l_f c_{b_f}}{J_y} & \frac{-l_r k_{b_r}}{J_y} & \frac{l_r c_{b_r}}{J_y} \\ 0 & 0 & 0 & 0 & 1 & 0 & 0 & 0 \\ 0 & 0 & 0 & 0 & 0 & 0 & 1 & 0 \\ 0 & 0 & 0 & 0 & 0 & 0 & 0 & 0 \\ 0 & 0 & 0 & 0 & 0 & 0 & 0 & 0 \end{bmatrix}$$

$$z_o=[z_{w_f}-h_f \quad z_{w_r}-h_r \quad \ddot{z}_b \quad \ddot{\theta} \quad z_{b_f}-z_{w_f} \quad z_{b_r}-z_{w_r} \quad u_f \quad u_r] \tag{6.11}$$

$$C_2=\begin{bmatrix} 0 & \frac{-c_{b_f}-c_{b_r}}{M_b} & 0 & \frac{l_f c_{b_f}-l_r c_{b_r}}{M_b} & \frac{-k_{b_f}}{m_b} & \frac{c_{b_f}}{M_b} & \frac{-k_{b_r}}{M_b} & \frac{c_{b_r}}{M_b} \\ 0 & \frac{l_f c_{b_f}-l_r c_{b_r}}{J_y} & 0 & \frac{-l_f^2 c_{b_f}-l_r^2 c_{b_r}}{J_y} & \frac{l_f k_{b_f}}{J_y} & \frac{-l_f c_{b_f}}{J_y} & \frac{-l_r k_{b_r}}{J_y} & \frac{l_r c_{b_r}}{J_y} \\ \frac{-k_{w_f}}{m_{w_f}} & \frac{c_{b_f}}{m_{w_f}} & \frac{l_f k_{w_f}}{m_{w_f}} & \frac{-l_f c_{b_f}}{m_{w_f}} & \frac{k_{b_f}+k_{w_f}}{m_{w_f}} & \frac{-c_{b_f}}{m_{w_f}} & 0 & 0 \\ \frac{-k_{w_r}}{m_{w_r}} & \frac{c_{b_r}}{m_{w_r}} & \frac{-l_r k_{w_r}}{m_{w_r}} & \frac{l_r c_{b_r}}{m_{w_r}} & 0 & 0 & \frac{k_{b_r}+k_{w_r}}{m_{w_r}} & \frac{-c_{b_r}}{m_{w_r}} \\ 0 & 0 & 0 & 0 & 1 & 0 & 0 & 0 \\ 0 & 0 & 0 & 0 & 0 & 0 & 1 & 0 \\ 0 & 0 & 0 & 1 & 0 & 0 & 0 & 0 \end{bmatrix}$$

$$z_o=[\ddot{z}_b \quad \ddot{\theta} \quad \ddot{z}_{w_f} \quad \ddot{z}_{w_r} \quad z_{b_f}-z_{w_f} \quad z_{b_r}-z_{w_r} \quad \dot{\theta}] \tag{6.12}$$

$$D_{11}=\begin{bmatrix} -1 & 0 \\ 0 & -1 \\ 0 & 0 \\ 0 & 0 \\ 0 & 0 \\ 0 & 0 \\ 0 & 0 \\ 0 & 0 \end{bmatrix} \quad D_{12}=\begin{bmatrix} 0 & 0 \\ 0 & 0 \\ \frac{1}{M_b} & \frac{1}{M_b} \\ \frac{-l_f}{J_y} & \frac{l_r}{J_y} \\ 0 & 0 \\ 0 & 0 \\ 1 & 0 \\ 0 & 1 \end{bmatrix} \quad D_{21}=\begin{bmatrix} 0 & 0 \\ 0 & 0 \\ \frac{k_{wf}}{m_{wf}} & 0 \\ 0 & \frac{k_{wr}}{m_{wr}} \\ 0 & 0 \\ 0 & 0 \\ 0 & 0 \end{bmatrix} \quad D_{22}=\begin{bmatrix} \frac{1}{M_b} & \frac{1}{M_b} \\ \frac{-l_f}{J_y} & \frac{l_r}{J_y} \\ \frac{-1}{m_{wf}} & 0 \\ 0 & \frac{-1}{m_{wr}} \\ 0 & 0 \\ 0 & 0 \\ 0 & 0 \end{bmatrix}$$

6.3 PSD Graphs of Suspension Systems

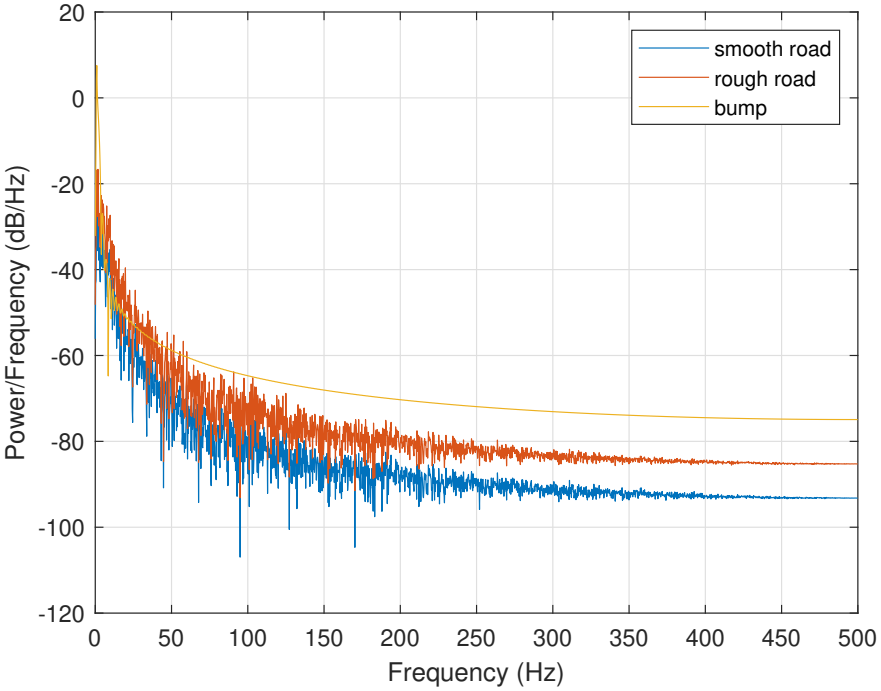

Figure 6.5: Passive suspension systems body linear acceleration PSD based on road profiles

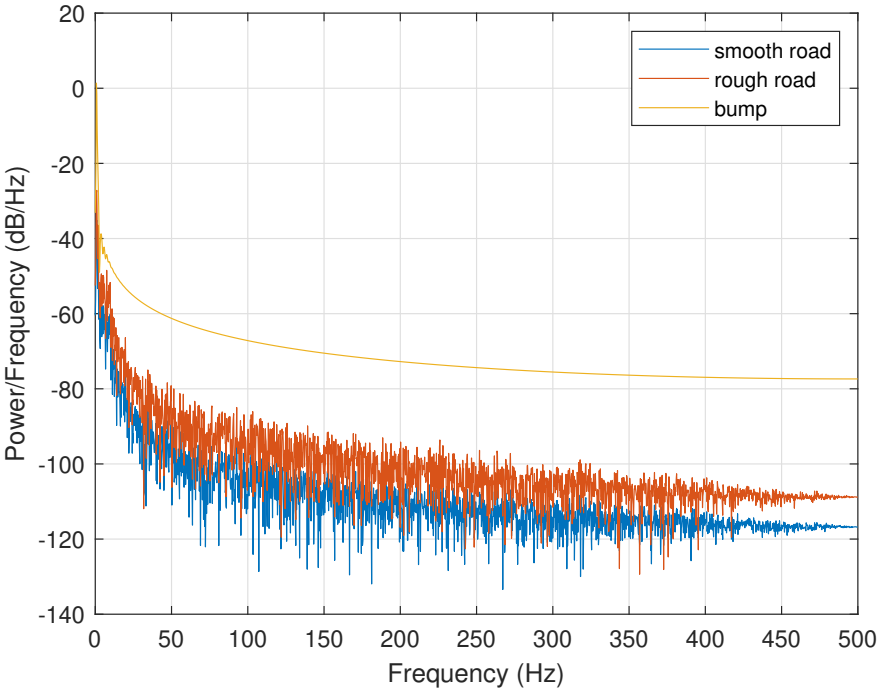

Figure 6.6: Passive suspension system body angular acceleration PSD based on road profiles

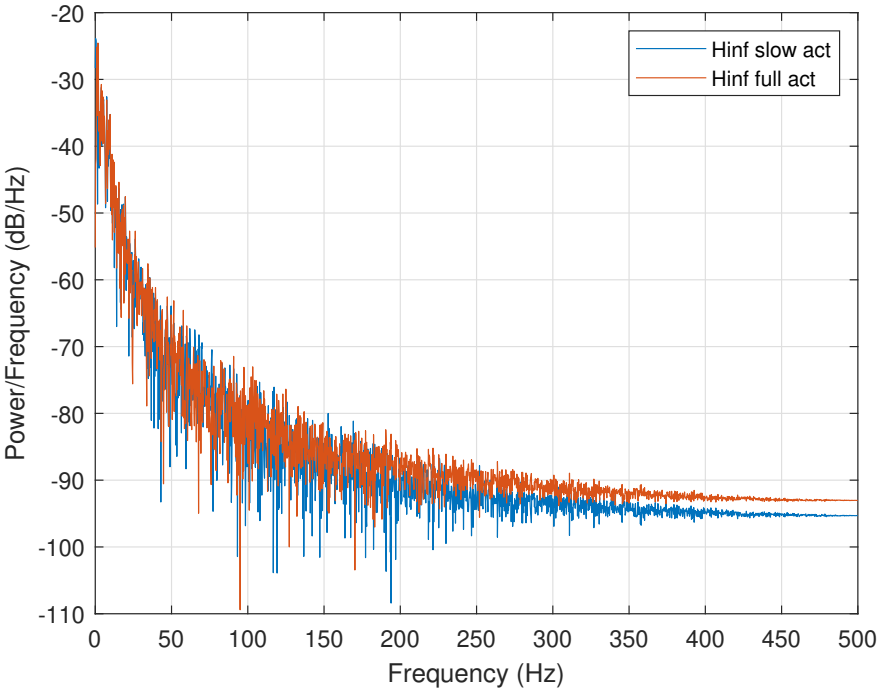

Figure 6.7: H_∞ control linear acceleration PSD graph on smooth road

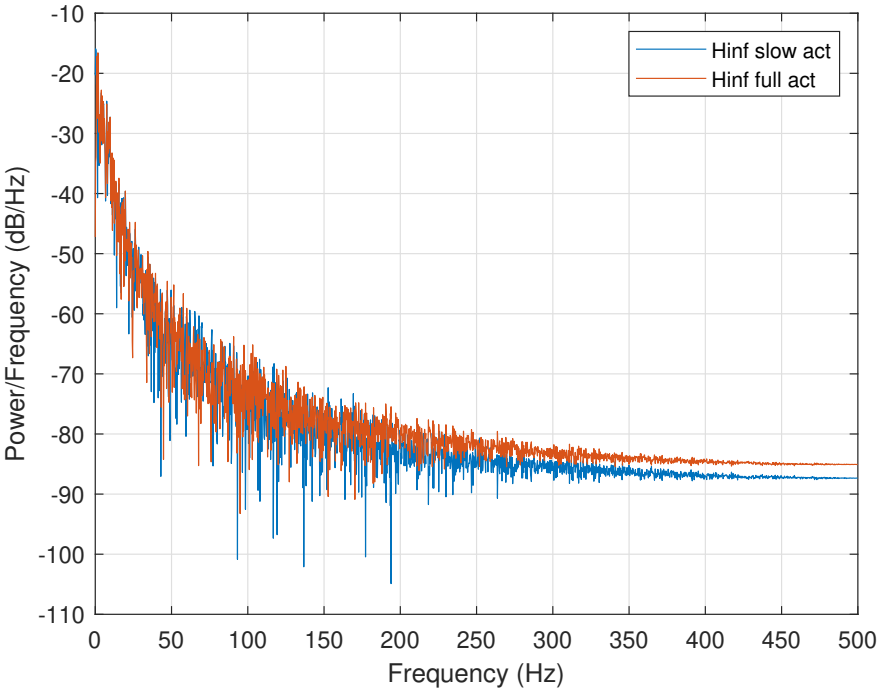

Figure 6.8: H_∞ control linear acceleration PSD graph on rough road

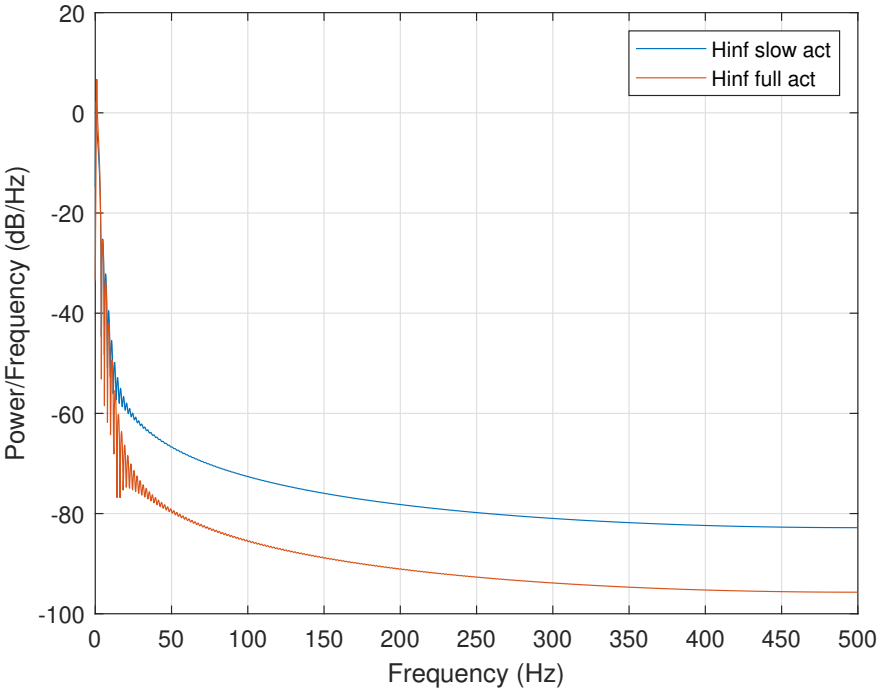

Figure 6.9: H_∞ control linear acceleration PSD graph on bump

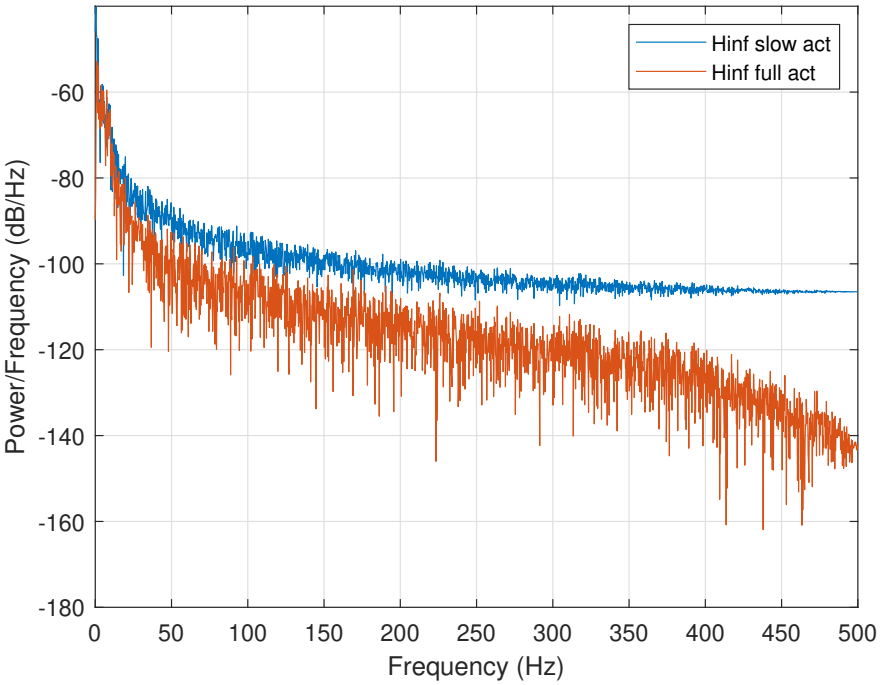

Figure 6.10: H_∞ control angular acceleration PSD graph on smooth road

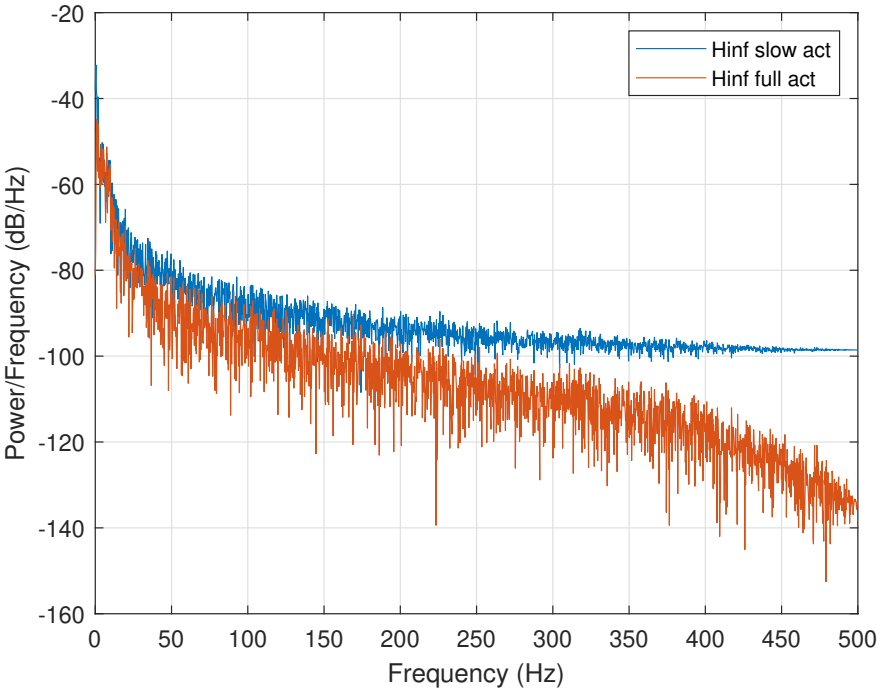

Figure 6.11: H_∞ control angular acceleration PSD graph on rough road

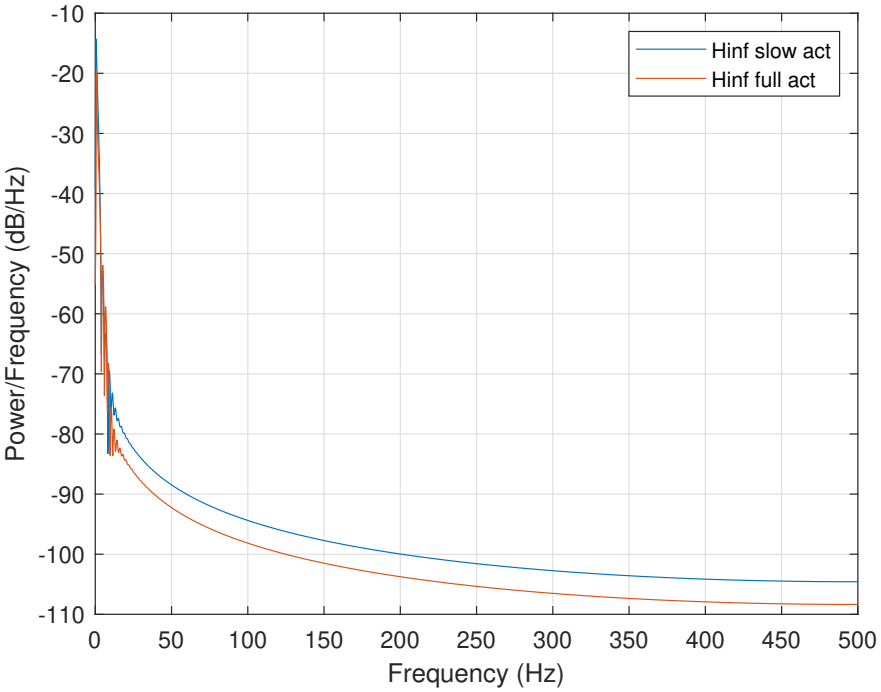

Figure 6.12: H_∞ control angular acceleration PSD graph on bump